Multivariate bias correction of high resolution regional climate change simulations for West Africa: performance and climate change implications

Diarra Dieng, Alex J. Cannon, Patrick Laux, Cornelius Hald, Oluwafemi Adeyeri, Jaber Rahimi, Amit K. Srivastava, Mamadou Lamine Mbaye, Harald Kunstmann

Angaben zur Veröffentlichung / Publication details:

Dieng, Diarra, Alex J. Cannon, Patrick Laux, Cornelius Hald, Oluwafemi Adeyeri, Jaber Rahimi, Amit K. Srivastava, Mamadou Lamine Mbaye, and Harald Kunstmann. 2022. "Multivariate bias correction of high resolution regional climate change simulations for West Africa: performance and climate change implications." *Journal of Geophysical Research: Atmospheres* 127 (5): e2021JD034836. https://doi.org/10.1029/2021JD034836.

JGR Atmospheres

RESEARCH ARTICLE
10.1029/2021JD034836

Multivariate Bias-Correction of High-Resolution Regional Climate Change Simulations for West Africa: Performance and Climate Change Implications

Diarra Dieng[1], Alex J. Cannon[2], Patrick Laux[1,3], Cornelius Hald[4], Oluwafemi Adeyeri[5], Jaber Rahimi[1], Amit K. Srivastava[6], Mamadou Lamine Mbaye[7], and Harald Kunstmann[1,3]

[1]Karlsruhe Institute of Technology (KIT), Campus Alpin, Institute of Meteorology and Climate Research - Atmospheric Environmental Research (IMK-IFU), Garmisch-Partenkirchen, Germany, [2]Environment and Climate Change Canada, Victoria, BC, Canada, [3]Augsburg University, Institute of Geography, Augsburg, Germany, [4]Meteorological Observatory Hohenpeißenberg, German Weather Service, Hohenpeißenberg, Germany, [5]School of Energy and Environment, City University of Hong Kong, Kowloon, Hong-Kong, [6]Institute of Crop Science and Resource Conservation, University of Bonn, Bonn, Germany, [7]Laboratoire d'Océanographie, des Sciences de l'Environnement et du Climat (LOSEC), Université Assane, SECK de Ziguinchor, Ziguinchor, Senegal

Key Points:

- Multivariate bias-correction (MBCn) of key meteorological variables accounting for their interdependency
- MBCn effectively removes the statistical biases as indicated by several measures and improves the representation of the probability density
- The corrected model ensemble mean preserves the climate change signal with a statistically significant change in precipitation

Supporting Information:

Supporting Information may be found in the online version of this article.

Correspondence to:

D. Dieng,
diarra.dieng@kit.edu

Citation:

Dieng, D., Cannon, A. J., Laux, P., Hald, C., Adeyeri, O., Rahimi, J., et al. (2022). Multivariate bias-correction of high-resolution regional climate change simulations for West Africa: Performance and climate change implications. *Journal of Geophysical Research: Atmospheres*, *127*, e2021JD034836. https://doi.org/10.1029/2021JD034836

Received 3 MAR 2021
Accepted 3 FEB 2022

Author Contributions:

Funding acquisition: Harald Kunstmann
Methodology: Alex J. Cannon, Cornelius Hald, Oluwafemi Adeyeri, Mamadou Lamine Mbaye
Project Administration: Harald Kunstmann
Supervision: Harald Kunstmann
Writing – original draft: Alex J. Cannon, Harald Kunstmann
Writing – review & editing: Patrick Laux, Oluwafemi Adeyeri, Jaber Rahimi, Amit K. Srivastava

Abstract A multivariate bias correction based on N-dimensional probability density function transform (MBCn) technique is applied to four different high-resolution regional climate change simulations and key meteorological variables, namely precipitation, mean near-surface air temperature, near-surface maximum air temperature, near-surface minimum air temperature, surface downwelling solar radiation, relative humidity, and wind speed. The impact of bias-correction on the historical (1980–2005) period, the inter-variable relationships, and the measures of spatio-temporal consistency are investigated. The focus is on the discrepancies between the original and the bias-corrected results over five agro-ecological zones. We also evaluate relevant indices for agricultural applications such as climate extreme indices, under current and future (2020–2050) climate change conditions based on the RCP4.5. Results show that MBCn successfully corrects the seasonal biases in spatial patterns and intensities for all variables, their intervariable correlation, and the distributions of most of the analyzed variables. Relatively large bias reductions during the historical period give indication of possible benefits of MBCn when applied to future scenarios. Although the four regional climate models do not agree on the same positive/negative sign of the change of the seven climate variables for all grid points, the model ensemble mean shows a statistically significant change in rainfall, relative humidity in the Northern zone and wind speed in the Coastal zone of West Africa and increasing maximum summer temperature up to 2°C in the Sahara.

1. Introduction

Future climate change projections over Africa show the likelihood of increased extreme weather conditions such as very hot days (when the maximum temperature exceeds 35°C), heat waves, and high fire-danger days (Engelbrecht et al., 2015; I. Niang et al., 2014; Vizy & Cook, 2012). Such changes may have a remarkable negative impact on climate-sensitive sectors if appropriate mitigation is not undertaken (e.g., Aich et al., 2014; Asseng et al., 2011; Knox et al., 2012; Lalou et al., 2019; Lobell et al., 2011; Sidibé et al., 2020; Sultan & Gaetani, 2016; Ulrike et al., 2016). Historical and future temperature increases, as well as future changes in precipitation patterns, can be highly variable at regional and local scales, with some regions becoming drier and others becoming wetter (Im et al., 2015). Understanding the regional signatures of climate variability and -change is especially important in West Africa due to its high natural climate variability and its low capacity to adapt to a changing climate. In the context of water resources, climate change and the increase of human water demands may cause a decline of the flow of the surface water sources by 20%–40% in 2050 in Western Africa (Misra, 2014).

In the context of agro-climate, crops, livestock, and pests are strongly dependent on the availability and the distribution of the water resources, the temperature (Sultan et al., 2019), and other climate variables (de Wit et al., 2005; de Wit & van Diepen, 2008). Hence, improved weather and climate forecast information, for example, in terms of characteristics of the rainy season (onset, cessation, rainfall amount) and the probability of extreme events (Dieng et al., 2018; Laux et al., 2008; Otto et al., 2017; Serdeczny et al., 2017; Waongo et al., 2015), could potentially lead to better farming and pastoral management. Maize, sorghum, and millet are widely produced in West Africa

and climate change may affect crop phenology, growth, and yield, and impede sustainable crop production in the future. Climate change is also projected to have a negative impact on the quantity and quality of feeds for livestock. More generally, linkages between meteorological conditions and agriculture have been investigated (Deser et al., 2012; Doto et al., 2015; Fisher et al., 2017; Greenstone & Greenstone, 2007; Mechiche-Alami & Abdi, 2020; A. Niang et al., 2017; Schlenker & Roberts, 2009; Sharon et al., 2013; Sultan et al., 2019; Sultan & Gaetani, 2016). Estimating this information in future climate projections is complex and involves reliable climate change scenarios with a credible representation of different hydro-climatological processes (Tall et al., 2018). Despite the recent progress in the development of general circulation models (GCMs), the Intergovernmental Panel on Climate Change (IPCC) indicates that GCMs still exhibit biases in their ability to simulate key features of the observed climate system (Randall et al., 2007). The move from global models to regional climate models (RCMs) represents a step forward in the ability to simulate details of local climate and climate change that cannot be resolved by coarser-resolution GCMs (Di Luca et al., 2012; Jie et al., 2013; Sheau et al., 2017). Sylla et al. (2015) illustrated the necessity of performing assessments of climate variability and future climate projections using multiple RCMs to estimate the response of the West African climate to global change. Thus, many studies in West Africa emphasize the importance of using multiple climate models to account for structural uncertainty when assessing climate change impacts on agriculture (Salack et al., 2012, 2015; Sultan et al., 2019), on water resources (Hagemann et al., 2013; Zhang et al., 2011) and Malaria predictability (Diouf et al., 2017).

To date, the majority of climate change assessments (e.g., Almazroui et al., 2020; Buontempo et al., 2015; Diallo et al., 2016; Diasso & Abiodun, 2017; Diedhiou et al., 2018; Dosio et al., 2015; Dunning & Allan, 2018; Heinzeller et al., 2018; Quenum et al., 2019; Sylla et al., 2016; Todzo et al., 2020) have investigated changes in precipitation and temperature rather than other meteorological forcing variables. In fact, omitting those other variables in climate impact models is likely to bias the predicted impacts of climate change on food security and agricultural development (Colston et al., 2018). The modeling study of de Wit et al. (2005) has highlighted the importance of taking into account surface solar radiation and its covariation with temperatures in estimating the impacts of temperature on crop yields. Wind affects the growth of crops in several ways, for example, by causing damage jointly with rain at the time of flowering or by increasing crop water requirements by increased evapotranspiration rates. Extremely high or low humidity may likewise affect yields. For example, relative humidity showed a statistically significant contribution to the yield of maize crop, but it negatively influenced the yield of other crops (Ali et al., 2017).

There is a lack of consensus in the future projection sign of mean and extreme climate conditions for West Africa (Akinsanola & Zhou, 2019; Dosio et al., 2020; Monerie et al., 2020; Nikiema et al., 2016; Ogega et al., 2020). Climate models fail to capture certain characteristics of present-day climate variability and these biases may be amplified when climate change effects are included, such as in agricultural climate impact assessments (Clark et al., 2016; Kauffeldt et al., 2016; Rosenzweig et al., 2014; Sidibé et al., 2020). If the climate change impact model is calibrated with inaccurate hydrometeorological data in the historical period, the impact of climate change can lead to wrong conclusions even if the climate change signal (CCS) itself is accurate.

For agricultural impact studies, Glotter et al. (2014) conclude that no climate model output can reproduce yields driven by observed climate unless a bias-correction is applied before. Therefore, bias-correction of RCM outputs is a necessary and indispensable prerequisite to the data being used in any climate change impact assessment (Ghosh & Mujumdar, 2009). The main goal of bias-correction is to adjust the statistical features (mean, variance) of RCM outputs in the historical period so that they are more similar to the observations (Ehret et al., 2012; Gudmundsson et al., 2012; Maraun, 2016; Teutschbein & Seibert, 2012a). Bias-correction of precipitation and temperature have traditionally received more attention (Laux, Rötter, et al., 2021; Piani et al., 2010; Watanabe et al., 2012). However, sunshine radiation, relative humidity, and wind speed likewise have significant biases in climate models. Various potential bias-correction techniques have been developed and used over the past decades, ranging from simple linear scaling to more skillful and advanced distribution matching methods (Ajaaj et al., 2016; Chen et al., 2019; Fang et al., 2015; Gutjahr & Heinemann, 2013; Iizumi et al., 2017; Lafon et al., 2013; Mehrotra & Sharma, 2016; Ojha et al., 2013; Piani et al., 2010; Singh et al., 2019; Teutschbein & Seibert, 2012b; Tiwari et al., 2016). For impact studies, quantile mapping (QM) or cumulative distribution function (CDF) transform approaches, which correct the entire distribution of a variable, are often recommended (Gudmundsson et al., 2012; Jie et al., 2013; Teutschbein & Seibert, 2012b). Promising results are obtained by Oettli et al. (2011) when applying the CDF transform (CDF-t) method (Colette et al., 2012) to climate model

Table 1
Characteristics of the WASCAL Regional Climate Models at (0.11°, 12 km) Employed in the Present Study

Driving GCM	GCM-center	RCM	Abbreviations
MPI-ESM-LR	Max Planck Institute for Meteorology	CCLM4.8.19	CCLM-M
MPI-ESM-MR	Max Planck Institute for Meteorology	WRF3.5.1	WRF-M
HadGEM2-ES	Met Office Hadley Center	WRF3.5.1	WRF-H
GFDL-ESM2M	National Oceanic and Atmospheric Administration	WRF3.5.1	WRF-G
Run	**CCLM**	**WRF**	
Radiation	Ritter-Geleyn, Ritter and Geleyn (1992)	RRTMG LW/SW	
Microphysics	Doms et al. (2011)	WSM5, Hong et al. (2004)	
Cumulus	Tiedtke, Tiedtke M (1989)	Grell-Dévényi, Grell and Devenyi (2002)	
Surface layer	Heise et al. (2003)	Janjic Eta, (Janjic, 1996, 2002)	
Land-surface scheme	TERRA-ML, Doms et al. (2011)	Noah LSM	

outputs. In particular, the authors showed that means and standard deviations of simulated yields of sorghum in Senegal are much more realistic with bias-corrected climate variables than those using raw climate model outputs. However, this approach, like other QM methods is univariate, that is, it corrects each climate variable independently from each other. Studies that have analyzed inter-variable aspects of bias-correction showed that univariate QM retains the inter-variable dependencies as represented by the raw climate model outputs (Ivanov & Kotlarski, 2017; Wilcke et al., 2013). But these may not correspond to the local inter-dependencies in observations. The interdependence of key climate variables, such as air temperature and precipitation, can be important when modeling crop yields. While rainfall affects plants photosynthesis activities and leaf area, temperature affects the length of the crop growing season (Hatfield & Prueger, 2015; Wheeler et al., 2000). To account for such interdependencies, multivariate bias-correction approaches need to be developed and applied.

Here, we present a bias-correction method that uses a non-parametric trend-preserving QM approach jointly with the multivariate bias-correction approach (MBCn, Cannon, 2018). It takes into account the interdependency between all climate variables during the historical (1980–2005) period and applies it to the near-future period (2020–2050). This study is limited to the near-future period (2020–2050) and the RCP4.5 since this period tends to be less sensitive to uncertainties related to RCP scenarios (IPCC 2013) and also due to our specific RCMs high-resolution climate runs from Heinzeller et al. (2018). Additionally, Sylla et al. (2016) reported that temperature changes from RCP4.5 and RCP8.5 start to diverge only from around 2050. The present work takes advantage of the high-resolution climate simulations of the West African Science Service Center on Climate Change and Adapted Land Use (WASCAL, e.g., Dieng et al., 2018; Dieng et al., 2017; Heinzeller et al., 2018) project. We further adapt, apply and analyze a post-processing bias-correction method of seven variables that are critical for climate impacts assessments: precipitation (Pr), mean near-surface air temperature (Tas), near-surface maximum air temperature (Tx), near-surface minimum air temperature (Tn), surface downwelling solar radiation (Rad), relative humidity (Rh, 2m), and wind speed (Wd, 10m). This study provides high-resolution regional and bias-corrected climate change information for West Africa. Results are relevant for any kind of agricultural, hydrological, or health climate change assessments in West Africa.

2. Materials and Methodology

2.1. RCM Data

The present work uses two regional climate simulation models: COnsortium for Small-scale MOdeling in CLimate Mode (CCLM) and Weather Research and Forecasting Model (WRF; see Table 1). The simulations cover the period 1980–2100 at 0.11° (12 km) spatial resolution over a domain of sufficient size to capture key large-scale circulation features that affect regional climate in West Africa including the displacement of the Intertropical Convergence Zone and the West African Monsoon (WAM). Comprehensive additional information about the domain setup, physical parameterizations, and boundary conditions are given in Dieng et al. (2017) and Heinzeller et al. (2018). We summarize the methodologies very briefly below (see Table 1), and refer the

reader to these publications. The regional climate projections are generated by applying a nested approach to two domains at 0.44° (50 km) and 0.11° (12 km) resolution. WRF uses a spectral nudging approach and the setup is based on the Klein et al. (2015) experiments which include 27 combinations of microphysics, planetary boundary layer, and cumulus parametrization schemes. Climate change projections have been created by downscaling the simulations of three global climate models, namely: MPI-ESM MR (Stevens et al., 2013), GFDL-ESM2M (Anon, 2012), and HadGEM2-ES (Jones et al., 2011). CCLM is driven by the lateral boundary conditions from the MPI-ESM LR (Stevens et al., 2013) and follows the COordinated Regional-climate Downscaling EXperiment domain setup (CORDEX; e.g., Giorgi & Gutowski, 2015; Nikulin et al., 2012; Panitz et al., 2014). Compared to those of the driving GCMs including MPI-ESM LR over the present climate, CCLM is found to add value over the regions affected by the WAM (Dosio et al., 2014).

2.2. Observed Data

Due to data-paucity, it is a challenge in Africa to gather multiple, homogeneous, temporally, and spatially consistent long-term observation-based hydro-meteorological series necessary for evaluating RCM simulations. For instance, by intercomparing different data sources and later validate with the RCMs, Panitz et al. (2014) and Sylla et al. (2012), reported substantial discrepancies among the different observational data sets. This makes it difficult to accurately assess the model performance. As a result, this study evaluates the bias-corrected model results against three observational data sets that is, two gauge-based gridded observational data sets; Climate Hazards Group Infrared Precipitation with Stations (CHIRPS; Funk et al., 2014) available at 0.05°spatial resolution and Climate Prediction Center (CPC; Fan & van den Dool, 2008) available at 0.5°spatial resolution. Additional rainfall data taken from the Multi-Source Weighted-Ensemble Precipitation (MSWEP; Beck et al., 2017) was used. Other data has been used for evaluation including the EWEMBI, which is the newly compiled reference data set employed for bias-correction in the ISIMIP2b (Inter-Sectoral Impact Model Intercomparison Project), and covers the entire globe at 0.5°spatial and daily temporal resolution from 1979 to 2013. EWEMBI is the combination of EartH2Observe forcing data (Calton et al., 2016), ERA-Interim reanalysis data (Dee et al., 2011), WATCH forcing data methodology applied to ERA-Interim reanalysis data (WFDEI; Weedon et al., 2014) and NASA/GEWEX Surface Radiation Budget data (Stackhouse et al., 2011).

Ground-based radiation, wind speed and relative humidity data sets over West Africa are sparse and not publicly available. We used ERA5 reanalysis in addition to the EWEMBI product for bias-correction validation.

The ERA5 data were aggregated to a daily time step and the 12 km model simulations were interpolated to ERA5 grid for comparison. Thereby, precipitation was re-gridded by using a first order conservative interpolation technique (Schulzweida, 2019) and by bilinear interpolation technique for temperatures, relative humidity, wind speed, and surface downwelling solar radiation.

2.3. The Bias-Correction Approach

For bias correction, we apply both methods from Cannon (2018) and Cannon et al. (2015).

First, a univariate QM (for the present period) based on an empirical distribution (QME) is applied to correct the systematic distributional error relative to historical ERA5. QM equates the observed and modeled CDFs via the transfer function constructed using information from the historical period exclusively; information provided by the future model projections is ignored.

Second, a relative and absolute change preserving the form of QM, Quantile Delta Mapping (QDM) from Cannon et al. (2015) is used to preserve the simulated relative changes in quantiles from future model projections. The algorithm combines two steps in sequence: first, the climate model's change signal (Delta) is removed from all projected future quantiles; second: the QM is then applied and the projected changes in quantiles are reintroduced to the bias-corrected model output.

Third, the multivariate bias-correction based on N-dimensional probability density function transform (Cannon, 2018) method is applied. The MBCn is a multivariate extension of QDM in which a random orthogonal rotation is applied to both climate model and observed data; the rotated marginal distributions are corrected using QDM, and the corrected variables are rotated back. This sequence of multivariate and univariate transformations

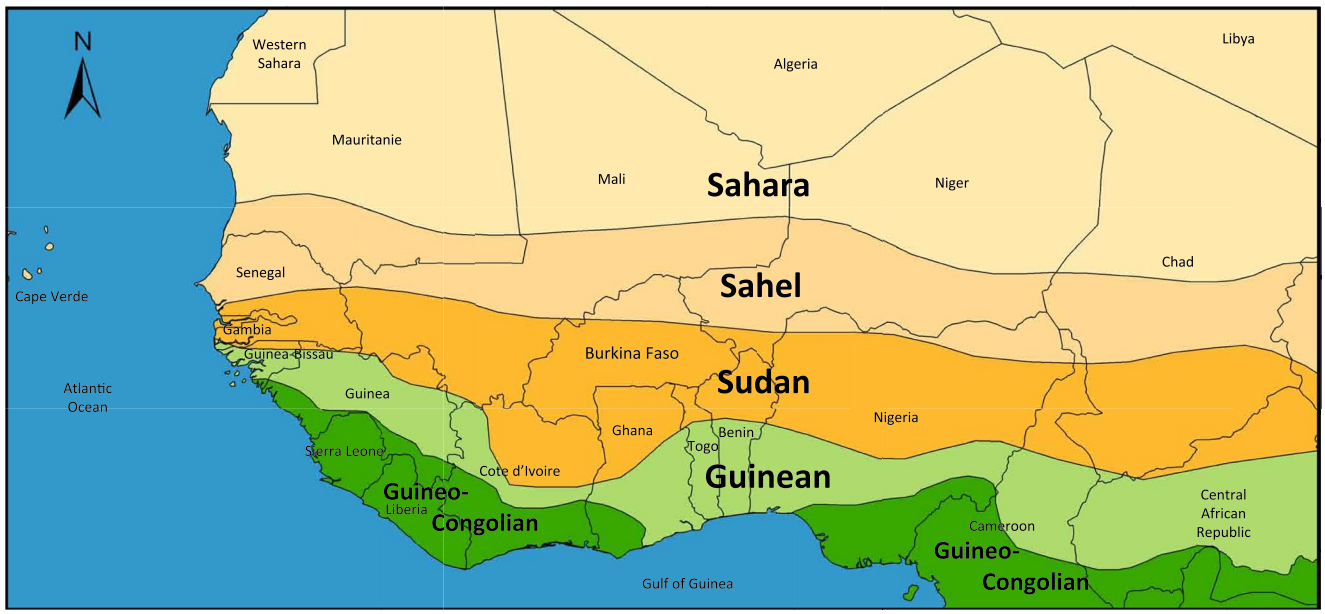

Figure 1. Map of West Africa with the focus on five investigated agroclimatic regions (source: CILSS, 2016).

is repeated until the corrected and observed multivariate distributions match. In this study, 100 iterations were conducted. MBCn has been applied in many studies, including Adeyeri et al. (2020) and Meyer et al. (2019).

2.4. Model Performance Indicators

We consider the five east-west belts which characterize the climate and vegetation in the following subregions in West Africa: Guineo-Congolian, Guinean, Sudan, Sahel, and Sahara, shown in Figure 1. By definition, our study area contains 5 climate zones that differ in terms of water availability, temperature, rainfall distribution, and amount during the growing season. The different agroclimatic conditions determine the possibility for rainfed agriculture.

We focus on the season from May to September, when cropping activity is at the maximum as referred by the United States Department of Agriculture and the International Production Assessment Division (https://ipad.fas.usda.gov/rssiws/al/crop_calendar/wafrica.aspx).

To assess model performance, we use a variety of validation measures. The selected model skill score (MSS, Equation 5) metric reflects height equally weighted components such as the normalized anomalies (r: standard deviation for model divided by observed standard deviation, Equation 1), the mean bias (B, Equation 2), the mean absolute error (MAE, Equation 3) and the index of agreement (d, Equation 4) as expressed in Adeyeri et al. (2020) and Gbode et al. (2019):

$$r = \frac{1}{(n-1)} \sum_{i=1}^{n} \left(\frac{M_i - \overline{M}}{\sigma_M} \right) \left(\frac{O_i - \overline{O}}{\sigma_O} \right) \tag{1}$$

$$B = \frac{1}{n} \sum_{i=1}^{n} (M_i - O_i) \tag{2}$$

$$MAE = \frac{1}{n} \sum_{i=1}^{n} |M_i - O_i| \tag{3}$$

$$d = 1 - \sum_{i=1}^{n} (M_i - O_i)^2 / \sum_{i=1}^{n} \left(|M_i - mean(O_i)| + |O_i - mean(O_i|)^2 \right) \tag{4}$$

$$MSS = (Sr_{\text{norm}} + (1 - |B|_{\text{norm}}) + (1 - SMAE_{\text{norm}}) + Sd_{\text{norm}} + tr_{\text{norm}} + (1 - tMAE_{\text{norm}}) + td_{\text{norm}}) \times 100 \tag{5}$$

Table 2
Relevant Indices for West-Africa (From Sultan et al., 2019)

	User-relevant indices	Description
Mean	Annual mean temp.	Annual mean surface temperature (°C)
	Annual max. temp.	Annual maximum surface temperature (°C)
	Annual min. temp.	Annual minimum surface temperature (°C)
	Annual wind speed	Annual mean wind speed (m/s)
	Annual relative humidity	Annual mean relative humidity (%)
	Annual solar radiation	Annual mean solar radiation (W/m^2)
	Annual rainfall	Total rainfall amount per year (mm/year)
Number of threshold exceedances	Annual rainy days	Number of days per year with rainfall above 1 mm
	Heavy rainfall events	Number of days per year with rainfall exceeding 30 mm/day
	Very heavy rainfall events	Number of days per year with rainfall exceeding 50 mm/day
	Rainfall intensity	Ratio between total annual rainfall and the number of rainy days
	Very hot days	Number of days per year with daily mean surface temperature

where O represents observation or reanalysis, M model output, σ standard deviation, and n number of data points in the series.

We additionally compute further agroclimatic indices shown in Table 2 that are relevant for agricultural applications in West Africa (Sultan et al., 2019).

A paired t-test (alpha = 0.05) was used to test whether there is a significant difference between observations, uncorrected, and bias-corrected WASCAL climate simulations. Considering that a common way to analyze changes in extremes is to follow the evolution of the percentiles of the daily climate data (Fischer & Knutti, 2016; Pendergrass & Knutti, 2018; Salack et al., 2018; Schär et al., 2016), a 99th percentile threshold is used to define extreme events over West Africa for the seven hydrometeorological climate variables considered.

3. Observational Uncertainty

Due to the spatio-temporal consistency in reanalysis products, several bias correction studies and related impact studies consider reanalysis or a combination from different sources (reanalysis, satellite, observations) as an alternative solution for validation studies over regions where observational data are sparse (e.g., Zhang et al., 2011). However, due to the highly spatial precipitation variability, it is mostly inaccurately estimated in reanalysis data due to its dependence on the type of assimilation method and model physics, thereby leading to uncertainty in the output, especially over West Africa. To circumvent this situation, precipitation variable from ERA5 reanalyses was evaluated against CHIRPS, CPC, and MSWEP to obtain a certain measure of consistency with the other data sets which are mostly rain-gauge based.

Figure 2 shows the observed probability distribution function (PDF) of precipitation for the dry (October–April) and wet months (May–September) over the different geographical areas.

The shape of ERA5 PDFs varies from region to region in similar ways to CHIRPS and MSWEP during the dry season. During the rainy period, the mean of the PDFs appears to be quite well represented in ERA5, with the largest similarities in the shape of the PDFs being over Sudan, Sahel, and Sahara. Over Guinean, we observe that the mean of daily ERA5 precipitation fields tends to be underestimated by less than 1 mm/day. Extreme rain events are well represented. ERA5 presents some uncertainty compared with CHIRPS for very small values of precipitation (<5 mm) over Guineo-Congolian which agrees with the findings of Quagraine et al. (2020). However, the ERA5 PDF usually falls into the observed range, meaning that, statistically, the ERA5 is able to reproduce the observed PDF despite a little uncertainty. It is shown that ERA5 brings extensive changes including higher

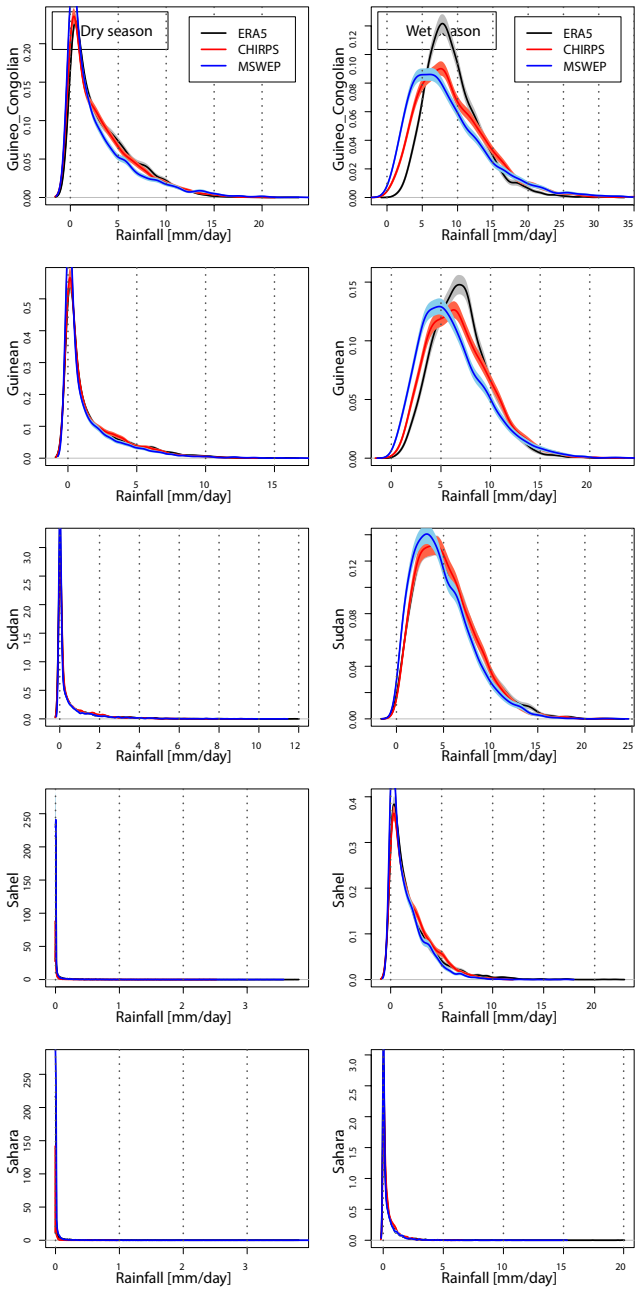

Figure 2. Probability density functions (PDF) of ERA5 seasonal rainfall for dry (October–April) and rainy (May–September) seasons in comparison with observations (CHIRPS and MSWEP) over the five climate land points during the historical period (1980–2005). The continuous lines belong to PDF average and the shading shows the first quartile (0.25) and the maximum (0.95) quartile.

spatial and temporal resolutions as well as a generally improved representation of, for example, precipitation (Gleixner et al., 2020). Another point of interest is that the result of the PDFs coincide with the spatial distribution of the differences in the average precipitation between ERA5, CHIRPS, CPC, and MWSEP (see Figure S1). The differences between ERA5 and CHIRPS are close to 0 in the dry period. The bias is mostly positive around 0.25 mm/day over the Guineo-Congolian and not statistically significant. Tarek et al. (2020) compared nine precipitation and two temperature data sets over 1,145 African catchments and they find that MSWEP, CHIRPS, and ERA5 outperformed the others for most catchments. ERA5 and CPC temperature data sets perform very similarly across all combinations, with ERA5 generally slightly outperforming CPC. Regarding radiation, relative humidity, and wind speed, more differences are evident between the data sets. This confirms the difficulty to quantitatively measure or/and estimate them since there are even notable differences among different reference data sets. EWEMBI shows higher surface downwelling solar radiation than ERA5 in both seasons due the improvement of total cloud cover simulation by ERA5 compared to that in ERA-Interim which are in turn part of the data sources of EWEMBI (Famien et al., 2018; Stackhouse et al., 2011).

4. Results

4.1. Evaluation of the MBCn Correction Method

The annual cycles of monthly precipitation sums from RCM outputs and the reference data sets (ERA5 and CHIRPS; Figure S2) are investigated over the selected regions. Considerable biases exist between the northern and southern parts of the study area. Values greater than 200 mm in the Guineo-Congolian and less than 50 mm over the rest of the domain are observed in the wet season of May–September, which ultimately discourages the direct application of RCM precipitation projections in local climate change assessments. Figure 3 shows the results of the comparative spatio-temporal performance of the multi-component scores MSS based on the individual model and ERA5 statistics over sub-domains and variables during the dry period (October–April) and the cropping period (May–September) during the historical period (1980–2005). Each climate zone is represented by the respective numbers: Guineo-Congolian (1), Guinean (2), Sudan (3), Sahel (4), and Sahara (5). We note that, for instance, there are some variables over some regions where the bias-corrected models have the best performance (high MSS values). In contrast, small improvements (lowest MSS) are seen after the bias-correction with values that generally does not exceed the 25% compared to the uncorrected performance. In general, corrections yield consistently higher validation scores during the wet season (cropping period) for CCLM-M, WRF-H, and WRF-M, and the dry period for WRF-G only. From October to March (dry season) with the bias-correction, CCLM-M shows a much better MSS performance for wind (+75%) compared to WRFs (difference ranging 10%–30%) but maximum temperature over the Sahel and Sahara, surface downwelling solar radiation and relative humidity over the whole domain do not show much improvement. Regarding the cropping period, CCLM-M and WRF-H are found to have good performance except for relative humidity and wind speed, respectively. More important is that the MSS is used to compare and rank the different model performances before and after bias-correction. The MSS ranges between 0% and 100% (100 for the best and 0 for the worst performing model). Based on the model rankings, WRF-G produces the lowest MSS despite the bias correction. A detailed technical description of these WRF model simulations is reported in Heinzeller et al. (2018). Overall, WRF-H indicates remarkable skills in reproducing the precipitation and temperature climatology, WRF-G being consistently colder

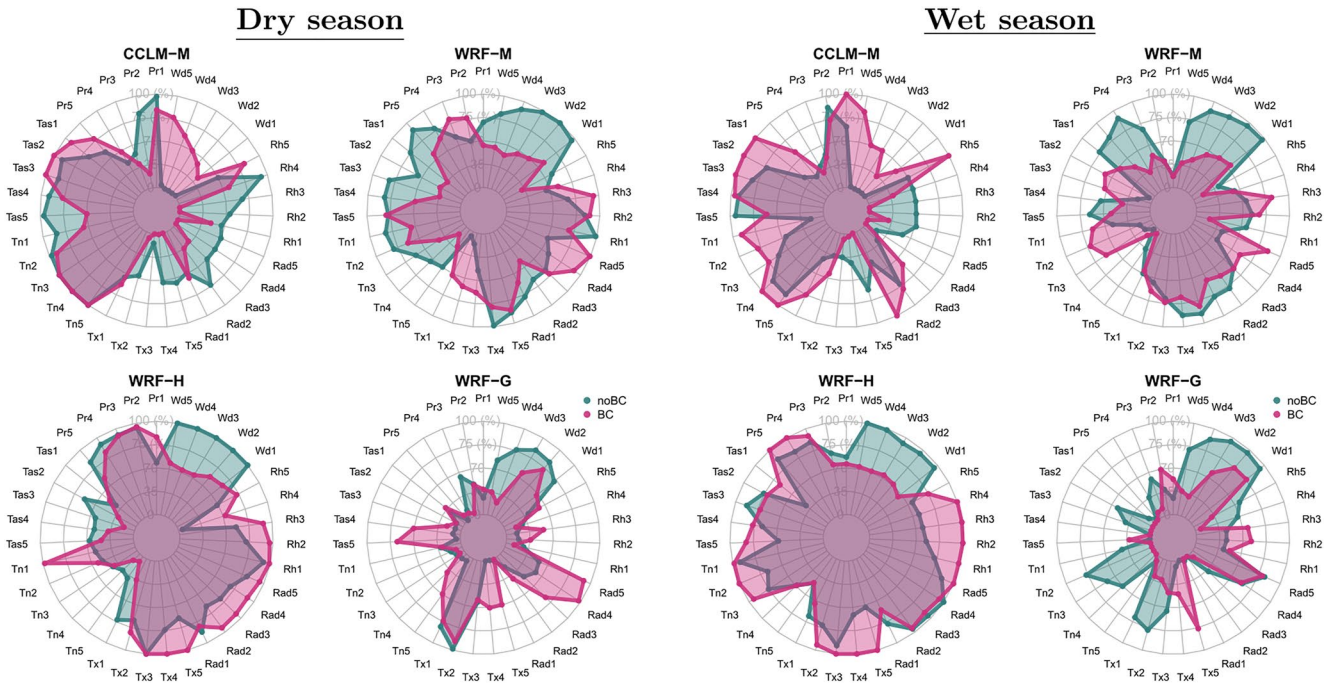

Figure 3. Spatio-temporal multi-component MSS index performance in dry period from September to April (left panel) and the cropping period from May to September (right panel) for rainfall (Pr), mean temperature (Tas), minimum temperature (Tn), maximum temperature (Tx), radiation (Rad), relative humidity (Rh) and wind speed (Wd) during the evaluation period (1980–2005). The included climatic zones are represented by a number: 1 = Guineo-Congolian, 2 = Guinean, 3 = Sudan, 4 = Sahel, and 5 = Sahara. noBC = uncorrected, BC = corrected.

with the lowest precipitation amount. In addition, some authors (e.g., Anon, 2012; Dunne et al., 2012; Elguindi et al., 2014) argue that the GFDL-ESM2M differ from observation and present small CCS due to the physical ocean component (ocean mean state). Based on the verification techniques, region of focus, and variables of interest, the combination of the characteristics of the forcing models and the complexity of physical parametrization have stronger influences on the representation of the different variables over the monsoon region (Flaounas et al., 2011; Gbode et al., 2019; Klein et al., 2015; Noble et al., 2014, 2017). Moreover, we quantify the uncertainties from the boundary conditions, that is, from the different driving GCMs (Figure S9) to highlight if and where substantial differences exist. It is found that apart from WRF-M, all RCMs show a relatively low sensitivity to the driving GCMs, which can be attributed to the effect of internal model physics (Gnitou et al., 2021; Laux, Dieng, et al., 2021).

Results from various studies (e.g., Diallo et al., 2012; Dosio et al., 2019; Gnitou et al., 2021; Saini et al., 2015) show that much of the regional-scale variability, which is resolved by the RCM, were not captured by the GCM. Consequently, the CCSs are better represented in RCMs than in GCMs (Diallo et al., 2012; Dosio et al., 2019; Gnitou et al., 2021; Saini et al., 2015).

To outline the performance of the applied bias-correction method, the validation is carried out by comparing individual RCM simulations with ERA5, CHIRPS, and CPC. The differences in the average precipitation, 2m temperature, and maximum temperature between the raw individual climate model and ERA5 (Figure S3) and the observations (CHIRPS and CPC) before and after error correction during the cropping period (May–September) are presented in Figure 4. The regions with dots mean significant variations ($p < 0.05$). We noticed that the bias-correction of the different average meteorological variables has improved significantly with good performance and confirmed in Table S1 in Supporting Information S1. Capturing the conditions preceding and during the cropping season plays a role in surface-related processes like soil moisture, which may alter in the context of agroclimate, crops, and livestock (Galmarini et al., 2019). The high bias or error in precipitation ranges between 2% and 20% (10 mm/day). The bias was substantially reduced after the bias-correction, with biases reaching values lower than 1 mm/day over large parts of the domain. Further results also demonstrate that the bias-correction does not affect the minimum precipitation values as much (see Table S1 in Supporting Information S1).

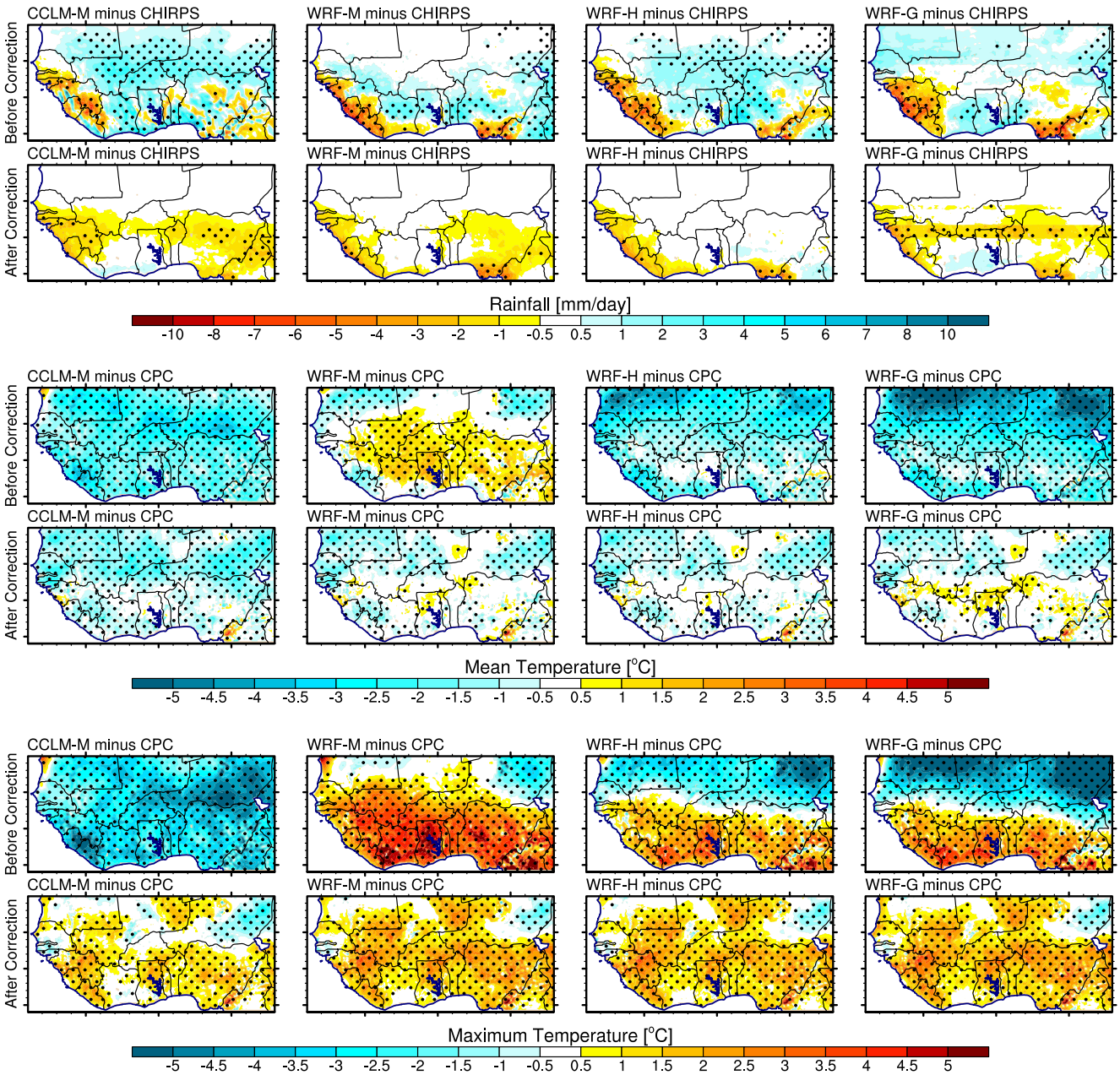

Figure 4. Mean bias of CCLM-M, WRF-M, WRF-H, and WRF-G for rainfall to CHIRPS, mean and maximum temperature to CPC before and after bias-correction for the cropping period (May–September) from 1980 to 2005. Statistically significant changes (*t*-test) at 95% confidence level are represented by black dots.

It can be concluded that the bias-correction for precipitation leads to good results. Previous research has shown that CCLM tends to simulate too far to the north the progression of the WAM (Dieng et al., 2018, 2017) and the bias-correction seems to correct for this bias reasonably well.

Before the bias-correction, temperature increase (overestimation) of around 0.5°C–5°C (in the order of 1.2%–3.5%) with daily mean temperatures greater than 35°C, daily maximum greater than 45°C and the minimum of 30°C are observed across almost all over the Saharan region. Across Guinean and Guineo-Congolian, temperature decrease (underestimation) of around 1.5°C–5.5°C (in the order of 5.7%–12.5%) is observed (Figure 4 and Figure S3). The MBCn-corrected mean temperature is slightly better for CCLM (−0.3%) than all WRF (1%–2.1%) in the North but is slightly worse over the coastal regions. The negative bias (before correction) becomes positive after correction. This is also confirmed by Adeyeri et al. (2020). While for the maximum temperature, the high

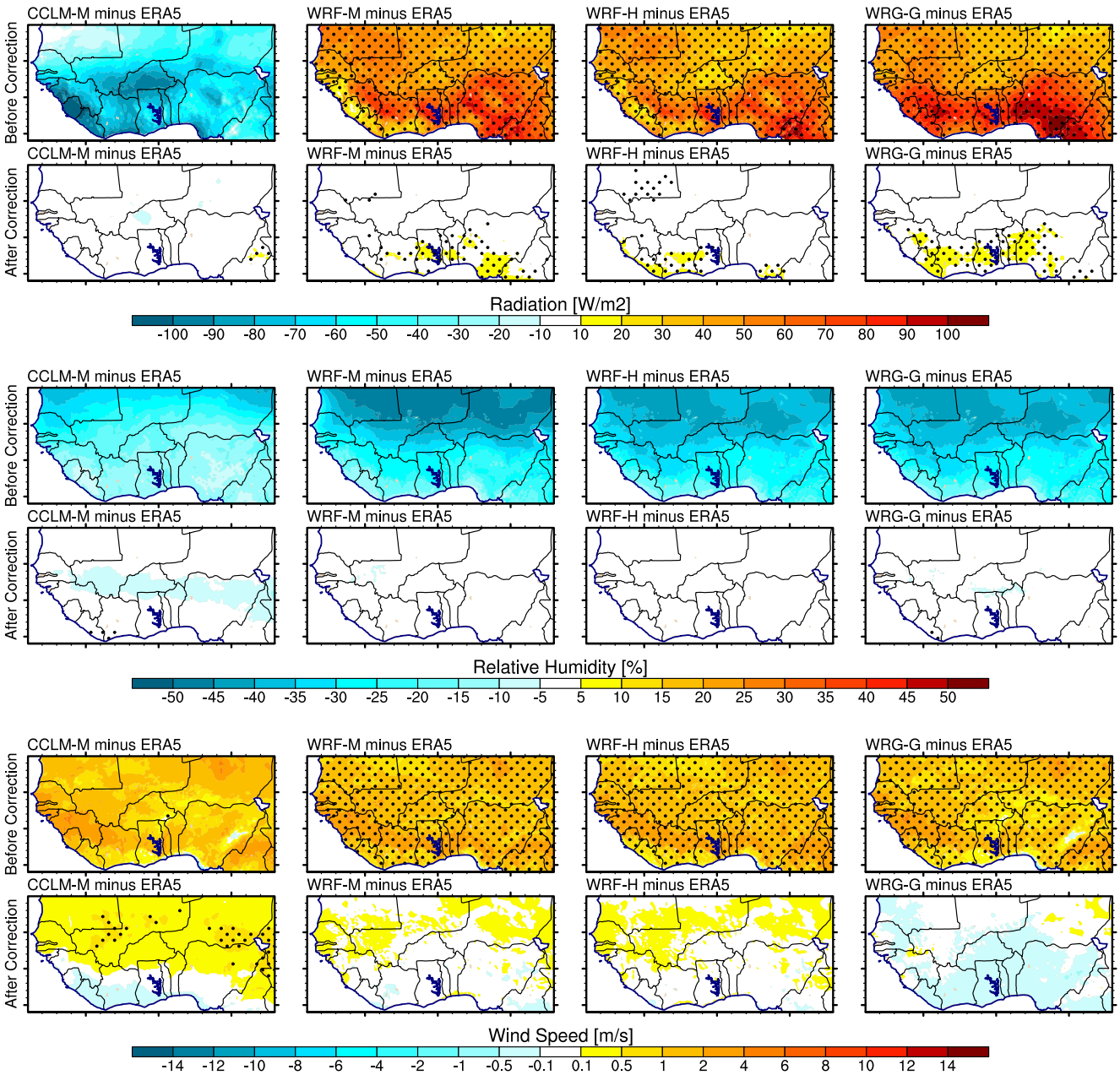

Figure 5. Mean bias of CCLM-M, WRF-M, WRF-H, and WRF-G for radiation, relative humidity and wind speed to ERA5 before and after bias-correction for the cropping period (May–September) from 1980 to 2005. Statistically significant changes (*t*-test) at 95% confidence level are represented by black dots.

warm bias in the coastal region (around 5°C) becomes less than 1°C. Differences in temperature have decreased significantly to values between −5°C and +2°C (before correction) to values between −2°C and 1°C. Corrections are smallest for the maximum temperature.

Near-surface wind speed, radiation and relative air humidity (Figure 5) also exhibit strong biases between uncorrected RCMs and ERA5 at every site ranging from −38% to 62% (up to 100 W/m^2 for radiation, −50% for relative humidity, and up to 16 m/s for wind speed), and in comparison to corrected simulations data the bias decline between −1% and 8.3%. The uncorrected relative humidity (Figure S4) is found to be better for most of the domain when compared with the EWEMBI. The bias-correction minimizes the difference between models and the EWEMBI drastically over Sudan, Sahel, and Sahara.

The overall area-weighted model ensemble mean difference with observations before bias-correction ranged from −7.58 to +2.32 mm/day for precipitation, from −4.4°C to 1.8°C for mean temperature, from −6.5°C to 3.4°C for maximum temperature, from −2.8°C to +2.8°C for minimum temperature, from −0.4 to +75 W/m^2 for radiation, from −43.9% to +13.5% for relative humidity and +2.2 to +6.6 m/s for wind speed. The average difference is satisfactorily reduced by bias-correction. This leads to an improved value from −3.5 to 0.6 mm/day for precipitation, −0.4°C to 1.0°C for mean temperature, of −1.3°C to 0.7°C for maximum temperature, of 0.1°C–2.4°C for minimum temperature, of −9.7 to +5.1 W/m^2 for radiation, of −4.3% to +0.6% for relative humidity and −0.25 to +0.29 m/s for wind speed. Model ensemble means outperform the individual RCMs and the driving GCMs because the different RCMs are characterized by different biases which partially offset each other in the ensemble average (Diallo et al., 2012). The MBCn-corrected model appears to have better reproduced the historical reference data in this respect.

Since local variations in rainfall, wind, temperature, and clouds are connected with the West African Monsoon system (Thorncroft et al., 2011), we extend the analysis of the previous results to investigate how the intercorrelation of different climate variables is represented (Figure S5). We represented the spatial distribution of the spearman rank correlation coefficient for different climate variables combinations Pr-Tas, Pr-rad, Rad-Tas, Rad-Rh, Tx-Tn, and Wd-Pr for the cropping period at the evaluation period. The climate model ensemble mean vs. the ERA5 is used as an example to demonstrate the results. There is a significant negative relationship (correlation coefficient is −0.1 to −0.7, p-value = 0.05) between temperature and rainfall, radiation and relative humidity; and wind and rainfall in North Africa. There is a significant positive relationship (correlation coefficient is +0.2 to +0.6, p-value = 0.03) between radiation and precipitation, relative humidity and radiation; and minimum and maximum temperature. In addition, all different combinations show RMSE values between 0.05 and 0.15 (results not shown) after error correction. The MBCn method has the capability to correct the simulated correlation coefficients and is able to represent the joint dependencies. Figure 6 shows the spatial Taylor diagrams (as expressed in RMSE, R, and SD) for the time-averaged MBCn methods applied to all RCMs during the evaluation period (1980–2005) for each climatic region of West Africa. In general, the four models have similar skill scores during the evaluation period. However, this is dependent on the climate zone. Results show that MBCn considerably improves RCM simulations as RMSE values clearly decrease, SD values get closer to observations and R values get higher. Nonetheless, in most regions, the extent of improvements is fairly comparable. Higher correlation values (between 0.90 and 0.99) and lower RMSE values (0–0.25) are achieved after bias-correction for most climatic regions, as also observed by François et al. (2020). Uncorrected precipitation, relative humidity, and wind speed are lower than their bias-corrected counterparts, suggesting that bias-corrected values better represent the temporal and spatial patterns of these respective variables over West Africa. Meyer et al. (2019) used MBCn to investigate the bias-correction effect in hydrological impact studies. They showed that MBCn-corrected GCM-RCM data caused more precipitation to fall as snow. The MBCn method improved the data correlation coefficients with better RMSE values of between 0.05 and 0.15 after bias correction. This agrees with previous studies, for example, Wilcke et al. (2013) and Zscheischler et al. (2019). Moreover, SD values of uncorrected RCM vary significantly across climatic regions, showing marked spatial and temporal heterogeneity. There is a tendency of larger spatial standard deviation in uncorrected wind speed and precipitation in the arid zone (Sahel and Sahara).

Table 3 shows the percentile values derived from historical WASCAL runs for the period from 1980 to 2005. Results show that the MBCn method successfully reduced the bias in extreme maximum temperature, relative humidity, and wind speed. However, there are still some inherent biases in precipitation and radiation. Additionally, MBCn led to more realistic results for precipitation during the historical reference period. In the water-limited Sudan, Sahel, and Sahara, the observed 99th percentile of rainfall events are overestimated from 15% (3 mm/day) to almost 83% (28 mm/day) and the bias-correction led to underestimated values ranging between 3% (0.8 mm/day) and 7% (0.5 mm/day). Over the Guinean-Congolian and Guinea regions, the MBCn has the lowest negative percentage bias of approximately −10% (5 mm/day) compared to high positive bias (61%, 20 mm/day) for the uncorrected case. Uncertainty in the bias-corrected extreme precipitation events is substantially smaller than that of uncorrected RCM precipitations (see Figure 7 and Figures S6 and S7). However, the overestimation of wet days (i.e., the number of wet days above a specific precipitation threshold), known as the drizzling effect (Gutowski et al., 2003) is very typical for dynamical models. Consistent with the previous results, we conclude that the MBCn bias-corrected results are much closer to the reference data sets than before the bias-correction, but in some cases of course do not perfectly match them. The non-synchronized internal climate variability

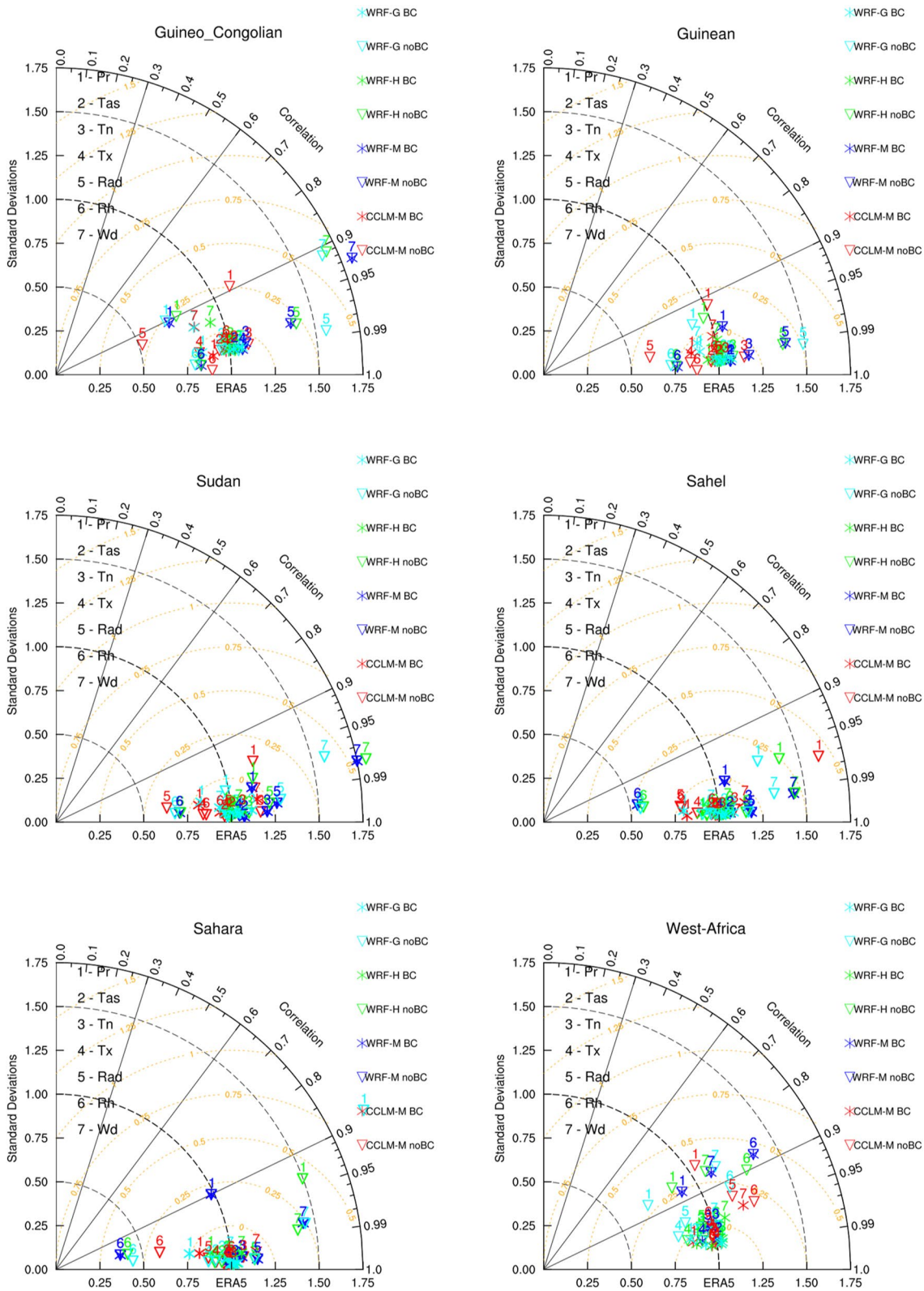

Figure 6. Taylor diagrams displaying a statistical comparison of RCMs and observation of the seven climate variables in evaluation runs (1980–2005) before (noBC) and after (BC) error corrections in the five investigated climate zones.

Table 3
Comparative Performance of the 99th Percentile for the Different Bioclimatic Zones From May to September During 1980–2005

Variables		Guineo	Guinean	Sudan	Sahel	Sahara
Pr(mm)	ERA5	**47.5**	**31.8**	**33.4**	**24.4**	**8.0**
	CHIRPS	**59.7**	**39.6**	**34.0**	**20.0**	**8.9**
	CCLM-M	**42.7**(66.3)	**30.1**(51.2)	**32.0**(61.1)	**23.6**(54.4)	**7.4**(24.4)
	WRF-M	4**5.3**(41.2)	**32.6**(48.4)	**33.5**(45.5)	**24.2**(23.7)	**7.6**(7.2)
	WRF-H	**44.7**(34.1)	**32.5**(40.2)	**33.6**(44.8)	**24.1**(28.7)	**7.6**(9.8)
	WRF-G	**46.1**(48.6)	**32.2**(48.2)	**32.8**(46.3)	**23.6**(28.1)	**7.1**(12.6)
Tas(°C)	ERA5	**27.4**	**31.8**	**32.4**	**35.7**	**36.5**
	CCLM-M	**27.3**(26.8)	**28.2**(28.6)	**32.1**(32.4)	**35.6**(35.8)	**36.5**(36.8)
	WRF-M	**28.0**(27.6)	**29.0**(29.5)	**32.9**(33.1)	**35.8**(36.4)	**36.5**(37.3)
	WRF-H	**27.7**(26.1)	**28.8**(27.9)	**32.8**(31.2)	**35.8**(33.5)	**36.5**(34.3)
	WRF-G	**28.1**(26.4)	**29.1**(27.8)	**33.0**(30.4)	**35.8**(32.7)	**36.6**(33.6)
Tx(°C)	ERA5	**32.9**	**34.1**	**38.2**	**43.1**	**44.3**
	CCLM-M	**32.3**(31.1)	**33.4**(33.8)	**37.5**(38.2)	**42.7**(41.9)	**44.3**(42.8)
	WRF-M	**33.3**(38.9)	**34.2**(37.6)	**38.3**(40.8)	**43.0**(43.9)	**44.4**(44.5)
	WRF-G	**33.1**(37.5)	**34.2**(36.1)	**38.2**(38.8)	**43.0**(41.0)	**44.4**(41.1)
	WRF-G	**33.3**(38.4)	**34.4**(36.2)	**38.3**(38.0)	39**.8**(43.0)	**44.38**(40.2)
Tn(°C)	ERA5	**22.6**	**23.3**	**26.8**	**29.7**	**30.5**
	CCLM-M	**23.3**(23.5)	**24.3**(24.3)	**27.9**(27.5)	**30.1**(30.6)	**30.5**(31.5)
	WRF-M	**23.57**(23.0)	**24.5**(24.2)	**28.4**(26.7)	**30.2**(29.9)	**30.5**(30.6)
	WRF-H	**23.3**(21.5)	**24.3**(22.6)	**28.3**(24.9)	**30.2**(27.5)	**30.5**(28.61)
	WRF-G	**23.6**(20.8)	**24.7**(22.0)	**28.5**(23.8)	**30.3**(26.5)	**30.5**(27.3)
Rad(W/m^2)	ERA5	**251.5**	**263.5**	**282.6**	**295.9**	**305.9**
	CCLM-M	**232.4**(244.5)	**253.0**(255.3)	**272.8**(275.9)	**292.2**(305.3)	**306.4**(318.3)
	WRF-M	**258.1**(318.1)	**263.1**(339.0)	**280.7**(357.1)	**367.2**(295.9)	**306.9**(369.1)
	WRF-H	**255.6**(311.8)	**259.7**(317.2)	**279.1**(3,324.8)	**295.8**(339.1)	**307.3**(348.2)
	WRF-G	**255.7**(325.3)	**259.2**(329.7)	**276.9**(340.3)	**294.7**(354.2)	**306.6**(362.9)
Rh(%)	ERA5	**98.7**	**98.3**	**97.6**	**95.1**	**89.6**
	CCLM-M	**98.7**(104.2)	**98.3**(101.7)	**97.6**(102.1)	**94.9**(96.9)	**89.4**(87.6)
	WRF-M	**98.6**(93.8)	**98.3**(90.3)	**97.6**(87.7)	**95.0**(73.4)	**89.3**(59.7)
	WRF-H	**98.7**(91.6)	**98.3**(87.6)	**97.6**(88.5)	**95.1**(77.2)	**89.3**(60.8)
	WRF-G	**98.7**(92.6)	**98.3**(88.3)	**97.6**(87.5)	**95.6**(74.7)	**89.4**(64.3)
Wd(m/s)	ERA5	**2.8**	**2.9**	**3.7**	**5.6**	**6.5**
	CCLM-M	**2.6**(16.9)	**3.0**(17.9)	**4.1**(19.7)	**6.1**(21.9)	**7.2**(21.7)
	CCLM-M	**2.7**(4.2)	**3.0**(6.5)	**3.8**(6.3)	**5.7**(7.8)	**6.7**(8.8)
	CCLM-H	**2.7**(4.6)	**2.9**(6.3)	**3.8**(6.2)	**5.7**(7.7)	**6.6**(8.3)
	CCLM-G	**2.6**(5.0)	**2.8**(6.4)	**3.6**(6.0)	**5.5**(7.9)	**6.6**(9.3)

Note. The MBCn values are bolded.

Table 4
Projected Future Mean Change (%) for the Different Climate Variables Over the Different Bioclimatic Zones During the Cropping Period (May–September) 2020-–050 Relative to the 1980–2005

Variables		Guineo	Guinean	Sudan	Sahel	Sahara
Pr	CCLM-M	−5.6	−6.4	−2.9	−14.8	−19.2
	WRF-M	3.0	9.2	15.6	12.5	38.7
	WRF-H	5.3	8.3	12.1	19.5	26.5
	WRF-G	4.8	4.8	3.7	4.5	9.4
Tas	CCLM-M	0.5	0.6	0.9	1.5	1.7
	WRF-M	1	1.0	1.0	0.9	0.9
	WRF-H	1.2	1.2	1.2	1.2	1.5
	WRF-G	1.0	1.0	1.0	1.2	1.2
Tx	CCLM-M	0.9	1.2	1.5	1.9	1.8
	WRF-M	0.8	0.9	0.9	1.0	1.1
	WRF-H	1.2	1.2	1.1	1.2	1.4
	WRF-G	1.0	1.2	1.2	1.2	1.3
Tn	CCLM-M	0.9	1.0	1.1	1.5	1.8
	WRF-M	1.1	1.1	1.1	1.1	1.2
	WRF-H	1.3	1.3	1.3	1.3	1.2
	WRF-G	1.1	1.1	1.1	1.2	1.2
Rad	CCLM-M	5.7	8.8	10.2	9.4	6.9
	WRF-M	−1.7	−1.0	−1.2	−1.3	−1.4
	WRF-H	−0.1	−0.7	−1.4	−1.5	−1.1
	WRF-G	1.3	1.5	1.2	0.6	0.2
Rh	CCLM-M	5.5	5.2	5.4	0.8	−1.4
	WRF-M	−0.1	−0.0	0.4	0.4	−0.0
	WRF-H	0.1	−0.1	0.3	1.4	1.5
	WRF-G	−02	−0.2	−0.0	−0.9	−1.3
Wd	CCLM-M	4.9	5.0	3.2	−0.7	−2.0
	WRF-M	2.4	2.1	1.4	0.6	0.5
	WRF-H	−1.7	1.7	2.2	4.1	4.2
	WRF-G	−1.9	−1.6	−0.4	0.6	−1.4

between the reference and simulated data sets can be one of the sources of the remaining bias (Cannon, 2016; Chen et al., 2020; Maraun et al., 2017; Maraun & Widmann, 2018).

5. Future Climate Change Signal

5.1. Results for Individual Simulations

Here, we investigate how the MBCn bias-correction method modulates the CCS of the seven climatic variables (see Section 2), which are essential for crop yields, livestock, hydrologic modeling, and the climate change impact assessment over West Africa. The CCS is for the scenario period 2020–2050 relative to the reference period 1980–2005. The predicted characteristics of future climate predicted results of four climate models in 2050 under RCP 4.5 during the cropping period (May–June–July–August–September) are presented in Figure 8 (Table 4). The results show that the projected precipitation changes differ between models. Indeed, projection studies based on GCMs and RCMs are mostly associated with model uncertainties due to the initialization and the parameterization schemes (Domínguez et al., 2010; Klein et al., 2015; Paxian et al., 2016; Tobin et al., 2013), the limited physical processes representation (Akinsanola & Zhou, 2019; Dosio et al., 2019; Saini et al., 2015; Stouffer et al., 2017) and the model dynamics (Diallo et al., 2012; Dosio et al., 2019; Monerie et al., 2020) which inevitably leads to uncertain and mixed results regarding the prospects of precipitation.

More recently, Monerie et al. (2020) investigated the causes of the uncertainties in simulating future changes in precipitation over the Sahel, using a set of 29 CMIP5 simulations and of 11 CMIP6 simulations. They found that the inter-model spread in precipitation change is mostly associated with model uncertainties in projecting changes in atmospheric circulation. By comparing large ensemble RCMs from the CORDEX including CCLM, Dosio et al. (2019) found that most regions and indices, where results are robust, are independent on the choice of the RCM or GCM.

Regarding the influence of the bias-correction on the CCS, Themeβl et al. (2012) point out that the bias-correction methods might falsify the original CCS of RCMs with extreme values being more strongly affected than the means. The bias-corrected RCMs reveal an increase in precipitation amount, as already observed by Oyerinde et al. (2017), ranging between 10% and 50% in most regions for WRF. A consistent increase in precipitation by more than 22% under RCP4.5 were reported by Ilori and Ajayi (2020), who used six RCMs CORDEX. Contrarily to WRF, CCLM shows a negative (decrease) projected precipitation change by up to −60% in the North and the Coastal regions. When comparing GCMs with RCMs (not shown), the results indicate that RCMs can change the signal projected by the forcing GCM across the Sahel region (8°W–2°E, 12°–17°N), where rainfall change is particularly sensitive to the representation of convection (Jackson et al., 2021). Systematic differences can be found between the two model groups in Figure 8. For instance, CCLM shows "dry" conditions, that is, projecting a decrease while WRF ("wet") is projecting an increase in mean precipitation. The possible mechanisms of the differences between the change in projected precipitation from WRF and CCLM can be delineated by analyzing the possible roles of (a) the changes in atmospheric circulation pattern (e.g., dynamic effect), as well as (b) the background moisture increase due to warming (e.g., thermodynamic effect) based on simplified moisture budget analysis at 850 hPa level following Dosio et al. (2020). In this respect, Jackson et al. (2021) conclude that the differences between projections of the WAM are fundamentally driven by differences in the diurnal cycles of rainfall, moisture convergence, and atmospheric humidity. According to the CCLM projections, mean precipitation is expected to decrease over large parts of the Sahel, mainly due to the decrease of horizontal moisture flux convergence. In addition, over the Guineo-Congolian and Guinean zones, this rainfall change from May to September is a consequence of the reduction in the

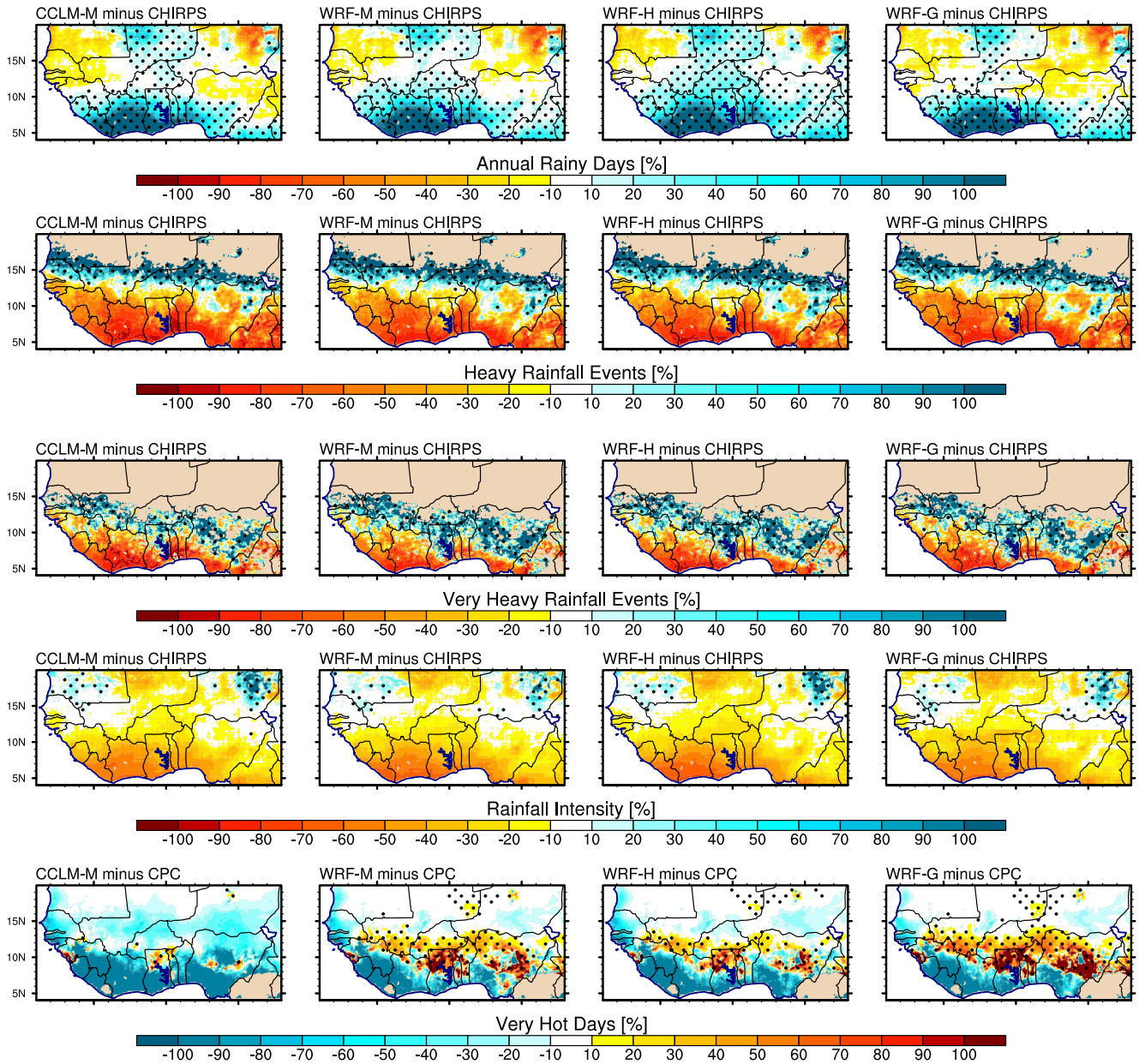

Figure 7. Bias (%) of CCLM-M, WRF-M, WRF-H, and WRF-G for the rainy days, the heavy rainfall events, the very heavy rainfall events, the rainfall intensity, and the very hot days to CHIRPS and CPC after error correction for the cropping period (May–September) from 1980 to 2005. Statistically significant changes (*t*-test) at 95% confidence level are represented by black dots.

number of rainy days, which, in turn, is positively correlated with the dynamic effect of the moisture budget. However, it is also demonstrated that the atmospheric circulation changes can affect precipitation changes, offsetting the thermodynamic contribution in the Sahel, as it is the case for the WRF simulations. This dynamic effect induces local divergence of horizontal moisture flux, resulting in marginal decreases of precipitation in the Sahel region. CCLM and WRF show different patterns of changes in mean and extreme precipitation over West Africa, which is caused by differences in dynamic contribution. This highlights the important role of atmospheric circulation changes in determining local responses in extreme precipitation.

For near-surface temperatures, despite the inherent uncertainties due to the climate model physics, the regionally downscaled climate models remain consistent in the CCS. The RCMs project an increase ranging between 1°C and 1.8°C whereas CCLM projected temperature tends to become more pronounced (up to 2.2°C) over the

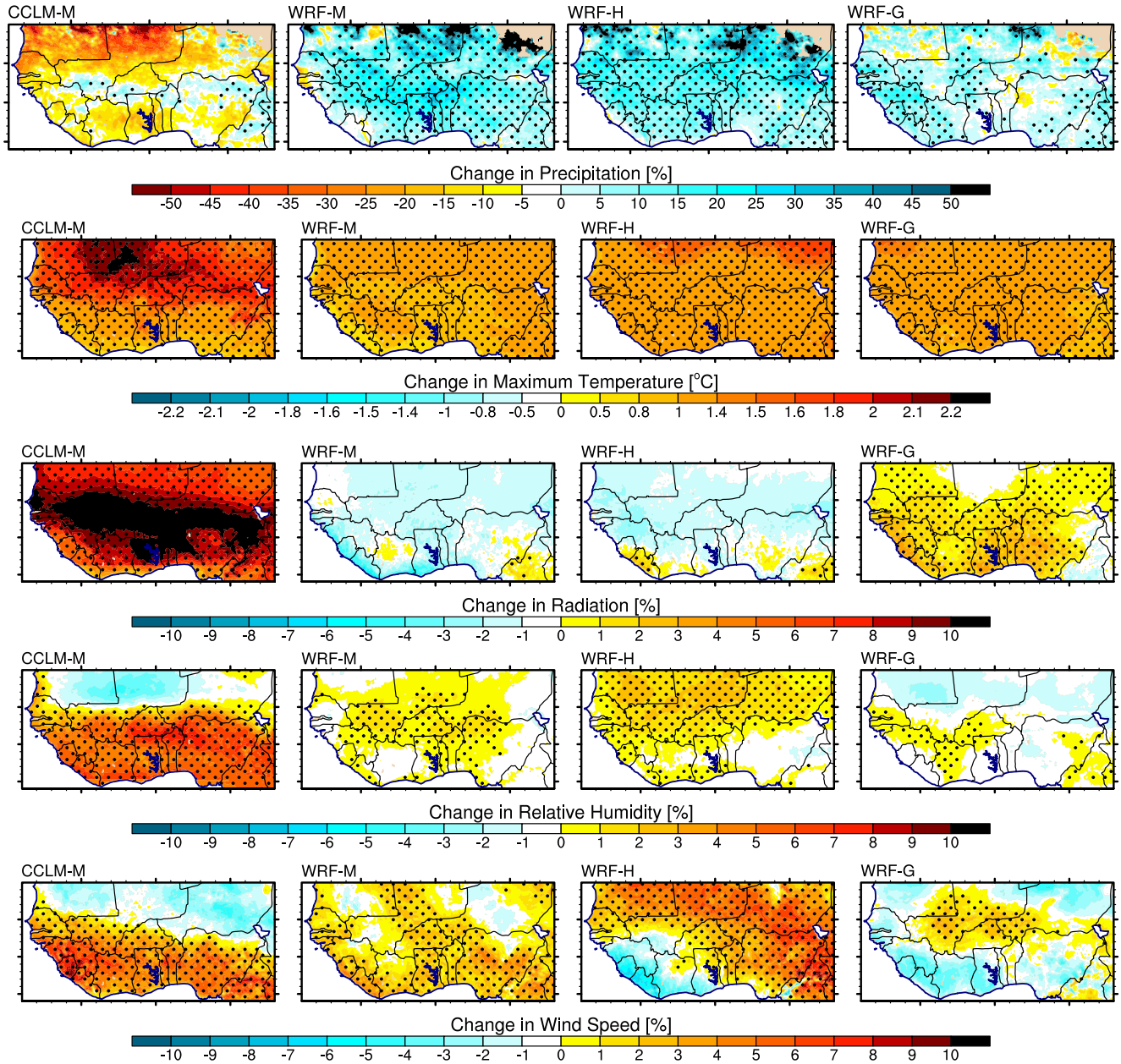

Figure 8. Mean projected relative change in mean precipitation, radiation, relative humidity, and wind speed, and absolute change in maximum temperature for the period 2020–2050 with respect to the historical period (1980–2005) using bias-corrected data from WASCAL-RCMs. The median of precipitation; maximum and minimum temperatures are shown in Table 4. Projected changes were estimated for the scenario RCP4.5 against the historical period on the season from May to September. Statistically significant changes (*t*-test) at 95% confidence level are represented by black dots.

Sahel and Sahara. Likewise, Botongho and Tog-Noma (2015) also noticed a temperature increase of 1.8°C under RCP4.5 in their study. The magnitudes of the changes are almost uniform for the whole study region except in WRF-M which exhibits changes of less than 1.5°C in most areas.

The expected change in radiation is a little higher for CCLM-M (about 12%, 50 W/m^2) as compared to WRF-G (about 6%, 10 W/m^2). An interesting case is CCLM, which underestimates radiation over the reference period, and subsequently projects a further increase in the future. The differences remain in the order of 6% of the uncorrected signal and the basic pattern of surface downwelling solar radiation change is not strongly altered by MBCn. This can be related to fact that model biases do not cancel each other out in the calculation of the CCS (Buser et al., 2009; Gobiet et al., 2015).

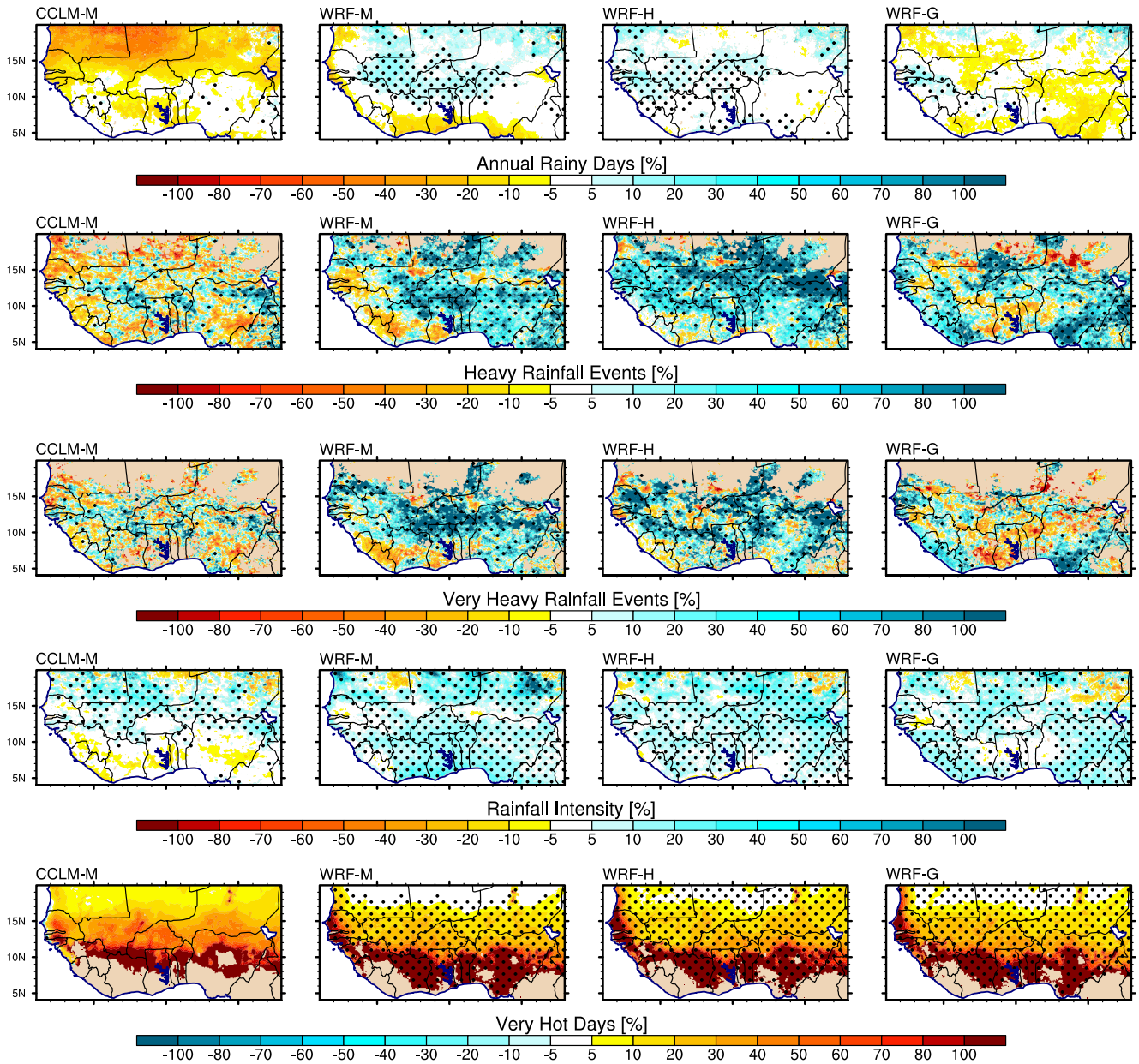

Figure 9. Percentage changes (%) in the annual rainy days, the heavy rainfall events, the very heavy rainfall events, the rainfall intensity, and the very hot days estimated against the historical reference period of 1980–2005 for the cropping period (May–September). Statistically significant changes (*t*-test) at 95% confidence level are represented by black dots.

The patterns of change in WRF-M and WRF-H show a radiation decrease of up to 5%, except for the Guineo-Congolian region for which the solar radiation is projected to increase by up to 5%.

Contrarily, previous studies conducted over West Africa (e.g., Bazyomo et al., 2016; Bichet et al., 2019) using regionally downscaled climate model outputs and the highest radiative forcing, predict a negative trend ranging from −0.03 to −0.11 W/m^2/year, but agree with our results on the whole distribution to warmer values suggesting the largest trend for temperature with a maximum value of 0.08 K/year. Wind speed conditions in 2020–2050 are fairly similar to baseline period conditions with an increase of up to 10%, while the magnitude of the change in surface wind speed varies from −0.5 to 0.1 m/s. Our results seem to confirm the findings from Akinsanola et al. (2021) and Sawadogo et al. (2019) although in our study most grid points exhibit projected increases in wind speed, rather than decreases as seen for WRF-G. Furthermore, Bichet et al. (2019) concluded that wind

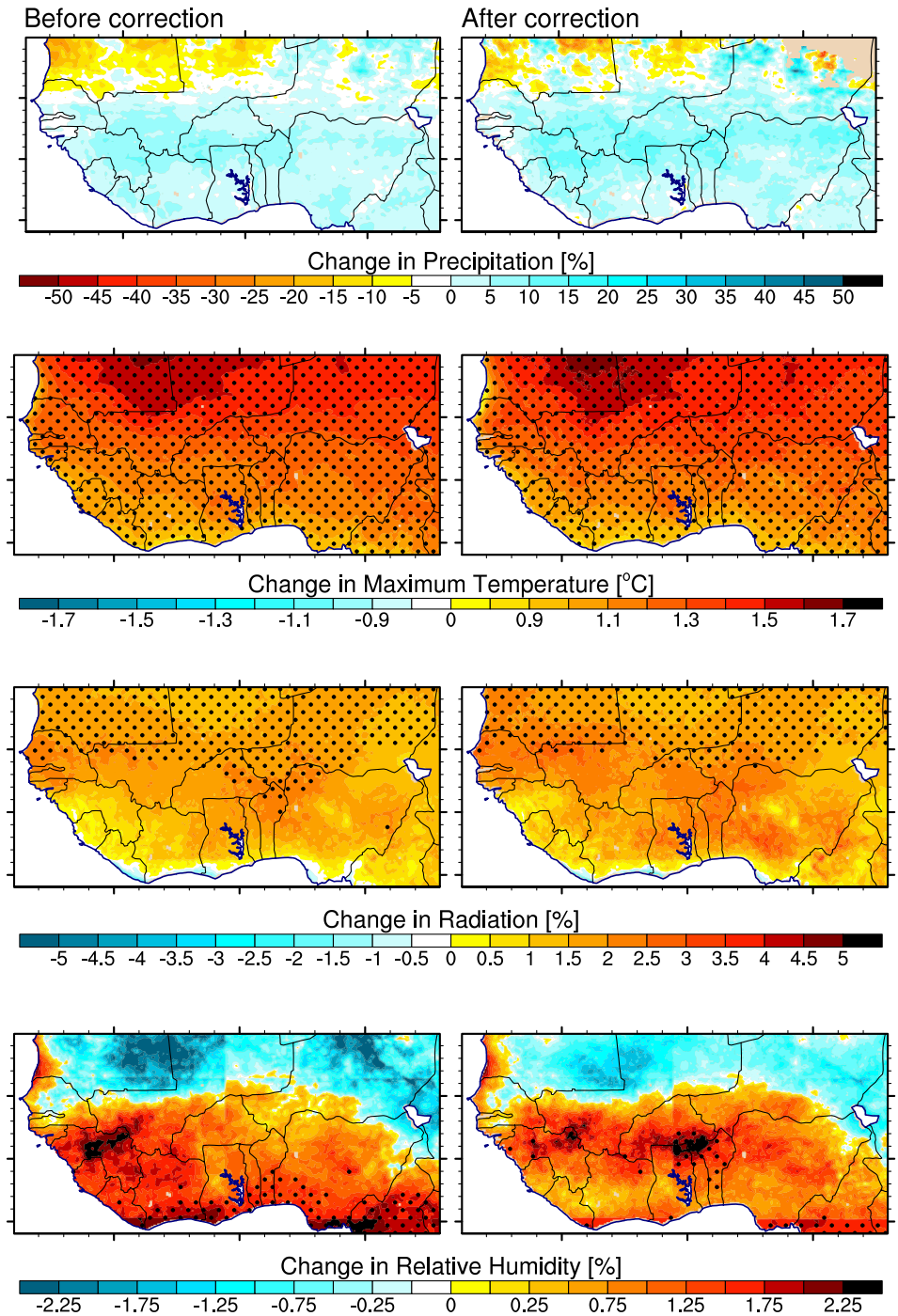

Figure 10. Mean projected relative change in model ensemble mean for the cropping period (May–September) in mean precipitation (%), radiation, relative humidity, and absolute change in maximum temperature for the period 2020–2050 with respect to the historical period (1980–2005) using bias-corrected data from WASCAL-RCMs. The median of precipitation; maximum and minimum temperatures are shown in Table 2. Projected changes were estimated for the scenario RCP4.5 against the historical period. Statistically significant changes (*t*-test) at 95% confidence level are represented by black dots.

speed is expected to increase everywhere by up to +8%. They suggested that the total uncertainty mostly results from model intervariability and GCM uncertainty. However, our results suggest that the bias-adjustments tend to enhance the CCS, especially for precipitation. Nevertheless, the change signals of the others climate variables are largely preserved after bias-correction, except for the maximum temperature over Sahel and Sahara, and the

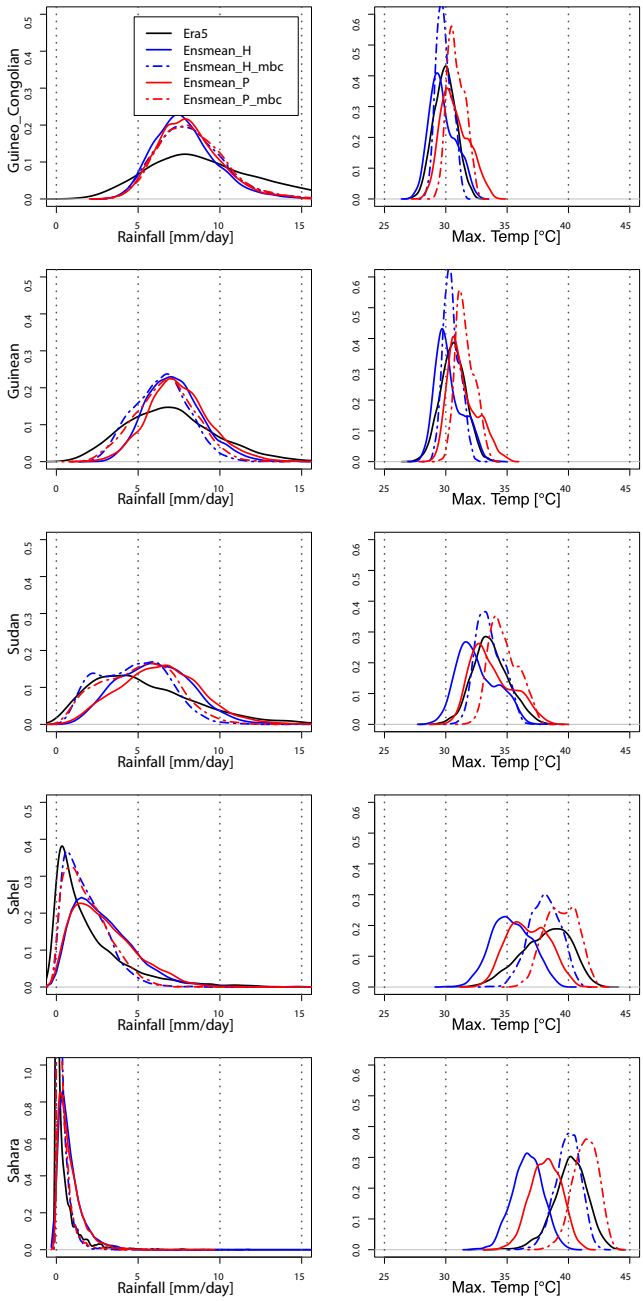

Figure 11. PDFs calculated from the ERA5 data set (black line), the model ensemble mean of the four model's before (continue lines) and after bias-correction (dotted lines) of daily precipitation, maximum temperature for the investigation areas. The first row shows Guineo-Congolian; the second row shows Guinean, the third row represents the Sudan, the fourth row presents the Sahel and the last row represents the Sahara. The blue lines are the model ensemble mean PDF for the historical climate (1980–2005) and red lines are for the projected climate (2020–2050).

radiation over Sudan and Sahel in CCLM. The bias-correction reduces the high maximum temperature values by up to 1°C and around 5% (25 W/m^2) the radiation. Thus, our results demonstrate that the CCS modification by bias-correction is a direct consequence of removing model biases, which was also suggested by Ivanov et al. (2018). RCP4.5 ranges of expected extreme precipitation changes span both negative and positive values, mostly between −30% and + 30% for the annual rainy days, −10% and 100% for both heavy and very heavy events, up to 40% for precipitation intensity (Figure 9). The increase in very hot days persists throughout the whole domain in all models. CCLM and WRF are consistent regarding the projections of the very hot days, which is similar to the findings of Fitzpatrick et al. (2020) and Nangombe et al. (2019). It must be noted that it is difficult to determine which predicted result is the most accurate among the four models in these five climatic regions as the individual models have very different behaviors.

5.2. Results for Model Ensemble Mean

Maraun (2012) suggested that multi-model ensembles need to be applied even after bias-correction when model sensitivities vary considerably in some regions. Therefore, the MBCn is applied to the model ensemble mean in Figure 10 to reduce the errors and consider the results as climate conditions till 2050.

The *t*-test between baseline (1980–2005) and future periods (2020–2050) shows a statistically significant change in rainfall, relative humidity in the Northern Zone, and wind speed in the Coastal Zone. Generally, precipitation mean values are projected to increase between 5% and 20%, in parallel to an increasing maximum temperature of up to 2°C in the Sahara, as also reported by Shiru and Park (2020). In addition, the results highlight a zonal contrast as illustrated by Sidibé et al. (2020) and the mean difference between projections and the historical period (2020–2050 minus 1980–2005) is expected to be 52, 42, 16, and 6 mm/day in Guineo-Congolian, Guinea, Sudan, and Sahara, respectively. This is also consistent with our results shown in Figure 11. Increases in minimum temperatures are projected to exceed those of maximum temperatures, which is in line with the analysis of Bamba et al. (2019). The increase of minimum temperature could be attributed to the higher atmospheric concentration of greenhouse gases which absorb and emit infrared radiation during the nights. The climate models suggest an increase in radiation of up to 5 W/m^2 and the distribution is more extended over the Western Sahel (Senegal and neighboring areas) than the rest of the domain. Using the CORDEX multi-model ensemble mean, Soares et al. (2019) found an increase in solar radiation of up to +15 W/m^2 (8%) with a band along the south Sahel, from Guinea to Ethiopia. The spatial correlation of the different climate variable changes are mostly positive in the range of 0.7–0.94 and statistically significant, indicating that the original spatial patterns of the changes are approximately kept. The multi-model ensemble mean (see Figure S8 shows a predominant increase in precipitation extremes accompanied by less amplification as compared to the individual raw RCM (<40%). These extreme conditions have the potential to increase flash floods and runoff (Roudier et al., 2014), reduce soil moisture (Diedhiou et al., 2018; Koné et al., 2020), and increase the risk of agricultural droughts (Mechiche-Alami & Abdi, 2020). However, it has to be mentioned that the bias-correction has the potential to alter the projected patterns of extreme precipitation and temperature; this is not limited to this study or region but has been shown for other works (e.g., Adeyeri

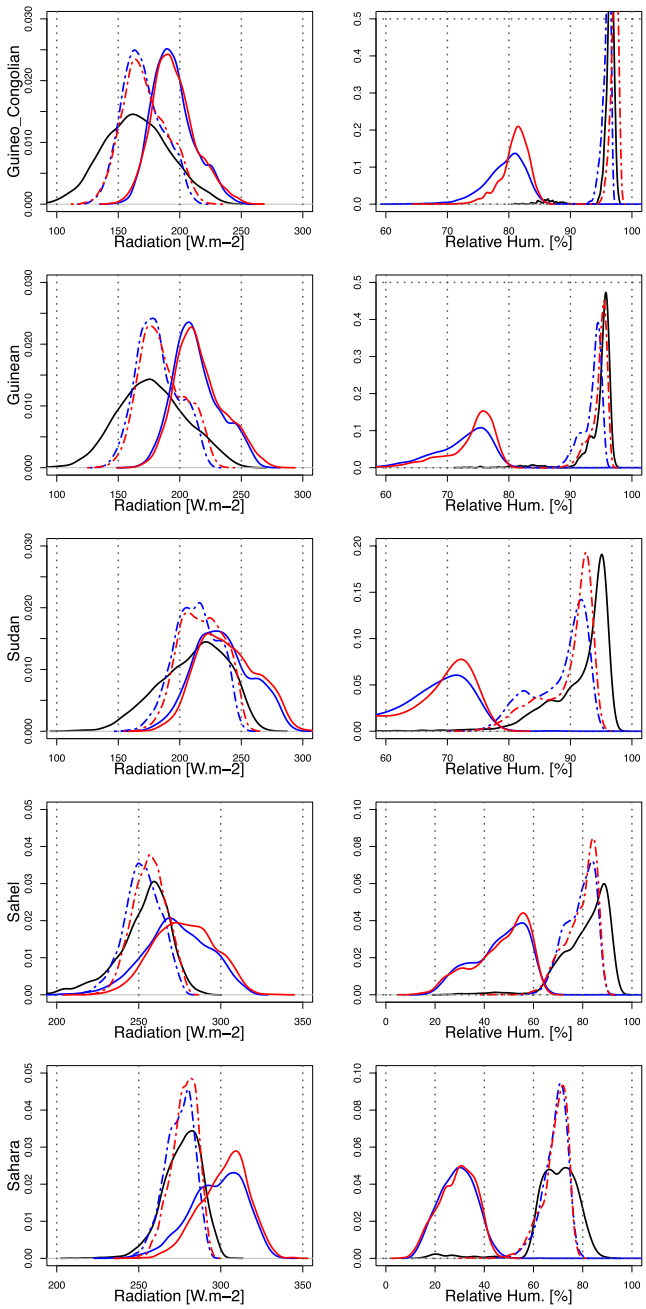

Figure 12. Same as Figure 11 but for surface downwelling solar radiation and relative humidity.

et al., 2020; Guo et al., 2018; Yin et al., 2020). The projected declines in precipitation and increases in temperature in Western Africa contribute to the decline in surface and groundwater availability and accessibility, affect the agriculture and hydrology sectors. Finally, the bias-correction is found to influence the PDFs of different climate variables (Figures 11 and 12), which also impacts the CCS. The shape of the PDF is generally conserved by the bias correction, for both regions and variables. As for the effect of the bias correction, it mainly affects the magnitude of the CCS rather than the direction of changes.

6. Summary and Concluding Remarks

This study is seeking an answer to the question: how does the bias-correction improve the climate variables and what are the implications for the derived future climate? We applied the multivariate bias correction by N-dimensional (MBCn) probability function transform method over the historical period (1980–2005) and future period (2020–2050) under RCP4.5 climate change scenario for seven variables that is, precipitation, mean near-surface air temperature, near-surface maximum air temperature, near-surface minimum air temperature, surface downwelling surface radiation, relative humidity, and wind speed. The MBCn bias-correction takes into account the dependency that exists between different variables. This is important, because some studies neglecting the variable's interdependency have demonstrated substantial consequences on future changes in multivariate extremes (Kirchmeier-Young et al., 2017; Zscheischler et al., 2019; Zscheischler & Seneviratne, 2017). In particular, we focused on the analysis of discrepancies between the raw model and bias-corrected model output to highlight regions where bias-correction algorithms might influence historical and projected climate data. The simulated present-day climate biases and validation for MBCn are first presented, followed by an analysis of the change signals. Evaluation of the results over five-agro climatic zones has been carried out on a list of priority user-based metrics (Sultan et al., 2019). According to the spatial distribution maps, the applied method is generally very effective at removing the biases and reducing considerably the biases of different measures even though the performance of the method varies across spatial and temporal scales. Results show higher uncertainty from the correction of precipitation density distributions than other analyzed variables for West Africa due to the high variability of precipitation in the region (Aloysius et al., 2016; Nikulin et al., 2012; Yira et al., 2017). The inability of climate models to capture certain characteristics is due to the biases directly inherited from the influence of GCM forcings or unrealistic large-scale variability, poor representation of internal variability, and imperfections in parameterization schemes and unresolved orography at the subgrid-scale orography (Eden et al., 2012; Ehret et al., 2012). This consequently affects the bias-correction performance because MBCn does not correct such effects. In Sudan and Sahel regions, where the correlation between temperature and precipitation is strongly negative, the MBCn mean temperature for wet months (May–September) is 0.5°C higher than the uncorrected data. On the other hand, poor bias-correction performance in adjusting the observed distribution of daily rainfall, mainly in the Guinean region over the historical period, affects the model's ability to reproduce varying extreme precipitation metrics. All sub-regions of West Africa are likely to experience a further decrease in annual precipitation and a further increase of extremes under RCP4.5. CCLM and WRF downscaling add value in terms of present-day climate simulations with improved resolution and are able to produce more reliable projection results at the regional scale. However, it should be noted that large uncertainties still exist in future projections. In general, the four RCMs do not agree on the same positive/negative sign of change in the magnitude of the seven climate variables for all

grid points covering the study area. In this study, CCLM and WRF are driven by MPI-ESM-LR, MPI-ESM-MR, GFDL-ESM2M, and HadGEM2-ES, respectively. To properly explain the difference of projections to the RCM itself or its driving GCM, the simulation of CCLM driven by GFDL-ESM2M and HadGEM2-ES is needed first. A multiple physical parameterization scheme ensemble as done in WRF is also needed by CCLM to fully cover the future climate change uncertainty. Second, WRF adopts an intermediate solution by conducting 11 yr time slice experiments to allows for a one-year spin-up of the soil conditions each time. Therefore as CCLM, a continuous run for WRF over the whole period is needed to fully cover the decadal variability.

The model ensemble mean shows a statistically significant mean change in rainfall, relative humidity in the Northern Zone, and wind speed in the Coastal Zone with increasing maximum summer temperature to 2°C in the Sahara region. The heavy and very heavy precipitation mean change show areas of alternating positive and negative changes moving from north to south, but a prevailing decrease in precipitation. Similarly, the mean and maximum temperature ensemble mean is projected to rise significantly across the northern Sahel, and Sahara regions respectively with a median increase of more than 3°C.

Caution has to be taken when correcting large geographical areas such as in our case here since the iterations permitted to reach convergence between model and observation need more computation time especially with more variables involved (Cannon, 2016). François et al. (2020) found that moving from a larger to a small domain consequently results in a good compromise between the number of iterations, the time needed for calculation, and the multivariable convergence. Also, the higher the number of dimensions to correct, the stronger the deterioration of rank chronology of the simulations (François et al., 2020). Even though the MBCn approach is applied over a big domain and over different climate zones in this study, future work needs to be more region-specific. Addressing these caveats by a more thorough analysis of constraints for multivariate bias-correction might further probe the possibilities and limitations of this method for analyzing climate-impact simulations over West Africa characterized by rainfed food crops. Hence, to fill the void, we first need to consider a large ensemble of downscaled GCMs climate simulation output. Second, we suggest to exclude simulations with severe and clearly demonstrated deficiencies (Herger et al., 2018; Maraun et al., 2017; Sippel et al., 2016) by using more representational observations data sets (Cortés-Hernández et al., 2016; Zscheischler & Seneviratne, 2017). Further investigations on a cross-validation protocol for MBCn bias-correction methods should be carried out for impacts that incorporate multiple, inter-dependent climate drivers as agricultural yields. Thus, the validation results could be analyzed and compared with a broad combination of indices to assess the added-value and/or any undesired effect of bias-correction.

Data Availability Statement

The raw RCM data can be obtained from https://doi.org/10.1594/PANGAEA.880512 (WRF) and from http://doi.org/10.5281/zenodo.1255882 (CCLM).

Acknowledgments
The authors are thankful to the UPSCALERS project (grant number AURG II-1-074-2016) which is part of the African Union Research Grants financed through the Financing Agreement between the European Commission and the African Union Commission (DCI-PANAF/2015/307-078). The authors would like to thank the *German Research Foundation* (DFG) through the *FOR 2936: Climate Change and Health in sub-Saharan Africa* project (grant number KU2090/14-1), and the KIT/IMK-IFU for providing computing resources at Linux cluster. The authors thank both Pangaea and Zenodo for hosting the model data. R-code for conducting the MBC is provided under GPL-2 license following https://CRAN.R-project.org/package=MBC. Open access funding enabled and organized by Projekt DEAL.

References

Adeyeri, O. E., Laux, P., Lawin, A. E., & Oyekan, K. S. A. (2020). Multiple bias-correction of dynamically downscaled CMIP5 climate models temperature projection: A case study of the transboundary Komadugu-Yobe river basin, Lake Chad region, West Africa. *SN Applied Sciences*, *2*(7), 1221. https://doi.org/10.1007/s42452-020-3009-4

Aich, V., Liersch, S., Vetter, T., Huang, S., Tecklenburg, J., Hoffmann, P., & Hattermann, F. F. (2014). Comparing impacts of climate change on streamflow in four large African river basins. *Hydrological Earth Systeme Science*, *18*(4), 1305–1321. https://doi.org/10.5194/hess-18-1305-2014

Ajaaj, A. A., Mishra, A. K., & Khan, A. A. (2016). Comparison of BIAS correction techniques for GPCC rainfall data in semi-arid climate. *Stochastic Environmental Research and Risk Assessment*, *30*(6), 1659–1675. https://doi.org/10.1007/s00477-015-1155-9

Akinsanola, A. A., Ogunjobi, K. O., Abolude, A. T., & Salack, S. (2021). Projected changes in wind speed and wind energy potential over West Africa in CMIP6 models. *Environmental Research Letters*, *16*(4), 044033. https://doi.org/10.1088/1748-9326/abed7a

Akinsanola, A. A., & Zhou, W. (2019). Projections of West African summer monsoon rainfall extremes from two CORDEX models. *Climate Dynamics*, *52*(3), 2017–2028. https://doi.org/10.1007/s00382-018-4238-8

Ali, S., Liu, Y., Ishaq, M., Shah, T., Abdullah Ilyas, A., & Din, I. U. (2017). Climate change and its impact on the yield of major food crops: Evidence from Pakistan. *Foods*, *6*(6), 39. https://doi.org/10.3390/foods6060039

Almazroui, M., Saeed, F., Saeed, S., Nazrul Islam, M., Ismail, M., Klutse, N. A. B., & Siddiqui, M. H. (2020). Projected change in temperature and precipitation over Africa from CMIP6. *Earth Systems and Environment*, *4*(3), 455–475. https://doi.org/10.1007/s41748-020-00161-x

Aloysius, N. R., Sheffield, J., Saiers, J. E., Li, H., & Wood, E. F. (2016). Evaluation of historical and future simulations of precipitation and temperature in central Africa from CMIP5 climate models. *Journal of Geophysical Research: Atmospheres*, *121*(1), 130–152. https://doi.org/10.1002/2015JD023656

Anon, A. (2012). GFDLś ESM2 global coupled climate-carbon Earth System Models. Part I: Physical formulation and baseline simulation characteristics. *Journal of Climate*, *25*, 6646–6665. https://doi.org/10.1175/JCLI-D-11-00560.1

Asseng, S., Foster, I., & Turner, N. C. (2011). The impact of temperature variability on wheat yields. *Global Change Biology*, *17*(2), 997–1012. https://doi.org/10.1111/j.1365-2486.2010.02262.x

Bamba, A., Diallo, I., Touré, N. E., Kouadio, A. K., Konaré, A., Dramé, M. S., et al. (2019). Effect of the African greenbelt position on West African summer climate: A regional climate modeling study. *Theoretical and Applied Climatology*, *137*(1), 309–322. https://doi.org/10.1007/s00704-018-2589-z

Bazyomo, S. D. Y. B., Agnidé Lawin, E., Coulibaly, O., & Ouedraogo, A. (2016). Forecasted changes in West Africa photovoltaic energy output by 2045. *Climate*, *4*(4), 53. https://doi.org/10.3390/cli4040053

Beck, H. E., van Dijk, A. I. J. M., Levizzani, V., Schellekens, J., Miralles, D. G., Martens, B., & de Roo, A. (2017). MSWEP: Three-hourly 0.25° global gridded precipitation (1979–2015) by merging gauge, satellite, and reanalysis data. *Hydrology and Earth System Sciences*, *21*(1), 589–615. https://doi.org/10.5194/hess-21-589-2017

Bichet, A., Hingray, B., Evin, G., Diedhiou, A., Kebe, C. M. F., & Anquetin, S. (2019). Potential impact of climate change on solar resource in Africa for photovoltaic energy: Analyses from CORDEX-AFRICA climate experiments. *Environmental Research Letters*, *14*(12), 124039. https://doi.org/10.1088/1748-9326/ab500a

Botongho, K., & Tog-Noma, P. E. (2015). *Modeling a Sahelian water resource allocation under climate change and human pressure: Case of Loumbila dam in Burkina Faso, (Unpublished doctoral dissertation)*. Cotonou, Benin: Université d'Abomey-Calavi.

Buontempo, C., Mathison, C., Jones, R., Williams, K., Wang, C., & McSweeney, C. (2015). An ensemble climate projection for Africa. *Climate Dynamics*, *44*(7), 2097–2118. https://doi.org/10.1007/s00382-014-2286-2

Buser, C. M., Künsch, H., Lüthi, D., Wild, M., & Schär, C. (2009). Bayesian multi-model projection of climate: Bias assumptions and interannual variability. *Climate Dynamics*, *33*(6), 849–868. https://doi.org/10.1007/s00382-009-0588-6

Calton, B., Schellekens, J., & Martinez-de la Torre, A. (2016). *Water resource reanalysis v1: Data access and model verification results. Earth System Science Data*. https://doi.org/10.5281/zenodo.57760

Cannon, A. J. (2016). Multivariate bias correction of climate model output: Matching marginal distributions and intervariable dependence structure. *Journal of Climate*, *29*(19), 7045–7064. https://doi.org/10.1175/JCLI-D-15-0679.1

Cannon, A. J. (2018). Multivariate quantile mapping bias correction: An N-dimensional probability density function transform for climate model simulations of multiple variables. *Climate Dynamics*, *50*(1), 31–49. https://doi.org/10.1007/s00382-017-3580-6

Cannon, A. J., Sobie, S. R., & Murdock, T. Q. (2015). Bias correction of GCM precipitation by quantile mapping: How well do methods preserve changes in quantiles and extremes? *Journal of Climate*, *28*(17), 6938–6959. https://doi.org/10.1175/JCLI-D-14-00754.1

Chen, J., Brissette, F. P., & Caya, D. (2020). Remaining error sources in bias-corrected climate model outputs. *Climatic Change*, *162*(2), 563–582. https://doi.org/10.1007/s10584-020-02744-z

Chen, J., Brissette, F. P., Zhang, X. J., Chen, H., Guo, S., & Zhao, Y. (2019). Bias correcting climate model multi-member ensembles to assess climate change impacts on hydrology. *Climate Change*, *153*(3), 361–377. https://doi.org/10.1007/s10584-019-02393-x

Clark, M. P., Wilby, R. L., Gutmann, E. D., Vano, J. A., Gangopadhyay, S., Wood, A. W., & Brekke, L. D. (2016). Characterizing uncertainty of the hydrologic impacts of climate change. *Current Climate Change Reports*, *2*(2), 55–64. https://doi.org/10.1007/s40641-016-0034-x

CILSS. (2016). *Comité permanent inter-états de Lutte contre la Sécheresse dans le Sahel; landscapes of West Africa-A window on a changing world: Ouagadougou (Tech. Rep.). 47914 252nd St, Garretson, SD 57030, United States*. U.S. Geological Survey EROS.

Colette, A., Vautard, R., & Vrac, M. (2012). Regional climate downscaling with prior statistical correction of the global climate forcing. *Geophysical Research Letters*, *39*(13). https://doi.org/10.1029/2012GL052258

Colston, J. M., Ahmed, T., Mahopo, C., Kang, G., Kosek, M., de Sousa Junior, F., & Zaitchik, B. (2018). Evaluating meteorological data from weather stations, and from satellites and global models for a multi-site epidemiological study. *Environmental Research*, *165*, 91–109. https://doi.org/10.1016/j.envres.2018.02.027

Cortés-Hernández, V. E., Zheng, F., Evans, J., Lambert, M., Sharma, A., & Westra, S. (2016). Evaluating regional climate models for simulating sub-daily rainfall extremes. *Climate Dynamics*, *47*(5), 1613–1628. https://doi.org/10.1007/s00382-015-2923-4

Dee, D. P., Uppala, S. M., Simmons, A. J., Berrisford, P., Poli, P., Kobayashi, S., & Vitart, F. (2011). The ERA-Interim reanalysis: Configuration and performance of the data assimilation system. *Quarterly Journal of the Royal Meteorological*, *137*(656), 553–597. https://doi.org/10.1002/qj.828

Deser, C., Phillips, A., Bourdette, V., & Teng, H. (2012). Uncertainty in climate change projections: The role of internal variability. *Climate Dynamics*, *38*(3), 527–546. https://doi.org/10.1007/s00382-010-0977-x

de Wit, A., Boogaard, H., & van Diepen, C. (2005). Spatial resolution of precipitation and radiation: The effect on regional crop yield forecasts. *Agricultural and Forest Meteorology*, *135*(1), 156–168. https://doi.org/10.1016/j.agrformet.2005.11.012

de Wit, A., & van Diepen, C. (2008). Crop growth modeling and crop yield forecasting using satellite-derived meteorological inputs. *International Journal of Applied Earth Observation and Geoinformation*, *10*(4), 414–425. https://doi.org/10.1016/j.jag.2007.10.004

Diallo, I., Giorgi, F., Deme, A., Tall, M., Mariotti, L., & Gaye, A. (2016). Projected changes of summer monsoon extremes and hydroclimatic regimes over West Africa for the twenty-first century. *Climate Dynamics*, *47*(12), 3931–3954. https://doi.org/10.1007/s00382-016-3052-4

Diallo, I., Sylla, M. B., Giorgi, F., Gaye, A. T., & Camara, M. (2012). Multimodel GCM-RCM ensemble-based projections of temperature and precipitation over West Africa for the early 21st century. *International Journal of Geophysics*, *2012*, 972896. https://doi.org/10.1155/2012/972896

Diasso, U., & Abiodun, B. J. (2017). Future impacts of global warming and reforestation on drought patterns over West Africa. *Theorical and Applied Climatology*, *133*(3–4), 647–662. https://doi.org/10.1007/s00704-017-2209-3

Diedhiou, A., Bichet, A., Wartenburger, R., Seneviratne, S., Rowell, D., Sylla, M., & Affholder, F. (2018). Changes in climate extremes over West and central Africa at 1.5°C and 2°C global warming. *Environmental Research Letters*, *13*(6), 065020. https://doi.org/10.1088/1748-9326/aac3e5

Dieng, D., Laux, P., Smiatek, G., Heinzeller, D., Bliefernicht, J., Sarr, A., & Kunstmann, H. (2018). Performance analysis and projected changes of agroclimatological indices across West Africa based on high-resolution regional climate model simulations. *Journal of Geophysical Research: Atmospheres*, *123*(15), 7950–7973. https://doi.org/10.1029/2018JD028536

Dieng, D., Smiatek, G., Bliefernicht, J., Heinzeller, D., Sarr, A., Gaye, A., & Kunstmann, H. (2017). Evaluation of the COSMO-CLM high-resolution climate simulations over West Africa. *Journal of Geophysical Research: Atmospheres*, *122*(3), 1437–1455. https://doi.org/10.1002/2016JD025457

Di Luca, A., de Elõa, R., & Laprise, R. (2012). Potential for added value in precipitation simulated by high-resolution nested regional climate models and observations. *Climate Dynamics*, *38*(5), 1229–1247. https://doi.org/10.1007/s00382-011-1068-3

Diouf, I., Rodriguez-Fonseca, B., Deme, A., Caminade, C., P Morse, A., Cissé, M., & Gaye, A. T. (2017). Comparison of Malaria simulations driven by meteorological observations and reanalysis products in Senegal. *International Journal of Environmental Research and Public Health*, *14*(10), 1119. https://doi.org/10.3390/ijerph14101119

Domínguez, M., Gaertner, M. A., de Rosnay, P., & Losada, T. (2010). A regional climate model simulation over West Africa: Parameterization tests and analysis of land-surface fields. *Climate Dynamics*, *35*(1), 249–265. https://doi.org/10.1007/s00382-010-0769-3

Doms, G., Förstner, J., Heise, E., Herzog, H., Mironov, D., Raschendorfer, M., et al. (2011). A description of the nonhydrostatic regional COSMO model. Part II: Physical Parameterization, *Deutscher Wetterdienst*, *154*, 161.

Dosio, A., Jones, R. G., Jack, C., Lennard, C., Nikulin, G., & Hewitson, B. (2019). What can we know about future precipitation in Africa? Robustness, significance, and added value of projections from a large ensemble of regional climate models. *Climate Dynamics*, *53*(9), 5833–5858. https://doi.org/10.1007/s00382-019-04900-3

Dosio, A., Panitz, H., Schubert-Frisius, M., & Lüthi, D. (2015). Dynamical downscaling of CMIP5 global circulation models over CORDEX-Africa with COSMO-CLM: Evaluation over the present climate and analysis of the added value. *Climate Dynamics*, *44*(9–10), 2637–2661. https://doi.org/10.1007/s00382-014-2262-x

Dosio, A., Panitz, H.-J., Schubert-Frisius, M., & Lüthi, D. (2014). Dynamical downscaling of CMIP5 Global circulation models over CORDEX-Africa with COSMO-CLM: Evaluation over the present climate and analysis of the added value. *Climate Dynamics*, *44*(9–10), 2637–2661. https://doi.org/10.1007/s00382-014-2262-x

Dosio, A., Turner, A. G., Tamoffo, A. T., Sylla, M. B., Lennard, C., Jones, R. G., & Hewitson, B. (2020). A tale of two futures: Contrasting scenarios of future precipitation for West Africa from an ensemble of regional climate models. *Environmental Research Letters*, *15*(6), 064007. https://doi.org/10.1088/1748-9326/ab7fde

Doto, V. C., Yacouba, H., Niang, D., Lahmar, R., & Agbossou, E. K. (2015). Mitigation effect of dry spells in Sahelian rainfed agriculture: Case study of supplemental irrigation in Burkina Faso. *African Journal of Agricultural Research*, *10*(16), 1863–1873. https://doi.org/10.5897/AJAR2015.9639

Dunne, J., John, J., Adcroft, A., Griffies, S., Hallberg, R., Shevliakova, E., & Zadeh, N. (2012). GFDL's ESM2 global coupled climate-carbon Earth System Models. Part I: Physical formulation and baseline simulation characteristics. *Journal of Climate*, *25*, 6646–6665. https://doi.org/10.1175/JCLI-D-11-00560.1

Dunning, C. M., Black, E., & Allan, R. P. (2018). Later wet seasons with more intense rainfall over Africa under future climate change. *Journal of Climate*, *31*(23), 9719–9738. https://doi.org/10.1175/JCLI-D-18-0102.1

Eden, J. M., Widmann, M., Grawe, D., & Rast, S. (2012). Skill, correction, and downscaling of GCM-simulated precipitation. *Journal of Climate*, *25*(11), 3970–3984. https://doi.org/10.1175/JCLI-D-11-00254.1

Ehret, U., Zehe, E., Wulfmeyer, V., Warrach-Sagi, K., & Liebert, J. (2012). HESS opinions "Should we apply bias correction to global and regional climate model data?" *Hydrological Earth Systeme Science*, *16*, 3391–3404. https://doi.org/10.5194/hess-16-3391-2012

Elguindi, N., Giorgi, F., & Turuncoglu, U. (2014). Assessment of CMIP5 global model simulations over the subset of CORDEX domains used in the Phase I CREMA. *Climate Change*, *125*, 7–21. https://doi.org/10.1007/s10584-013-0935-9

Engelbrecht, F., Adegoke, J., Bopape, M.-J., Naidoo, M., Garland, R., Thatcher, M., & Gatebe, C. (2015). Projections of rapidly rising surface temperatures over Africa under low mitigation. *Environmental Research Letters*, *10*(8), 085004.

Famien, A. M., Janicot, S., Ochou, A. D., Vrac, M., Defrance, D., Sultan, B., & Noël, T. (2018). A bias-corrected CMIP5 data set for Africa using the CDF-t method—A contribution to agricultural impact studies. *Earth System Dynamics*, *9*(1), 313–338. https://doi.org/10.5194/esd-9-313-2018

Fan, Y., & van den Dool, H. (2008). A global monthly land surface air temperature analysis for 1948-present. *Journal of Geophysical Research: Atmospheres*, *113*(D1). https://doi.org/10.1029/2007JD008470

Fang, G., Yang, J., Chen, Y., & Zammit, C. (2015). Comparing bias correction methods in downscaling meteorological variables for a hydrologic impact study in an arid area in China. *Hydrology and Earth System Sciences*, *19*(6), 2547–2559. https://doi.org/10.5194/hess-19-2547-2015

Fischer, E. M., & Knutti, R. (2016). Observed heavy precipitation increase confirms theory and early models. *Nature Climate Change*, *6*(11), 986–991. https://doi.org/10.1038/nclimate3110

Fisher, J. B., Melton, F., Middleton, E., Hain, C., Anderson, M., Allen, R., & Wood, E. F. (2017). The future of evapotranspiration: Global requirements for ecosystem functioning, carbon and climate feedbacks, agricultural management, and water resources. *Water Resources Research*, *53*(4), 2618–2626. https://doi.org/10.1002/2016WR020175

Fitzpatrick, R. G. J., Parker, D. J., Marsham, J. H., Rowell, D. P., Jackson, L. S., Finney, D., & Stratton, R. (2020). How a typical West African day in the future-climate compares with current-climate conditions in a convection-permitting and parameterized convection climate model. *Climate Change*, *163*(1), 267–296. https://doi.org/10.1007/s10584-020-02881-5

Flaounas, E., Bastin, S., & Janicot, S. (2011). Regional climate modeling of the 2006 West African Monsoon: Sensitivity to convection and planetary boundary layer parameterization using WRF. *Climate Dynamics*, *36*(5), 1083–1105. https://doi.org/10.1007/s00382-010-0785-3

François, B., Vrac, M., Cannon, A. J., Robin, Y., & Allard, D. (2020). Multivariate bias corrections of climate simulations: Which benefits for which losses? *Earth System Dynamics*, *11*(2), 537–562. https://doi.org/10.5194/esd-11-537-2020

Funk, C. C., Peterson, P. J., Landsfeld, M. F., Pedreros, D. H., Verdin, J. P., Rowland, J. D., et al. (2014). *A quasi-global precipitation time series for drought monitoring* (Vol. 832, p. 4). U.S. Geological Survey.

Galmarini, S., Cannon, A., Ceglar, A., Christensen, O., De Noblet, N., Dentener, F., & Zampieri, M. (2019). Adjusting climate model bias for agricultural impact assessment: How to cut the mustard? *Climate Services*, *13*, 65–69. https://doi.org/10.1016/j.cliser.2019.01.004

Gbode, I. E., Dudhia, J., Ogunjobi, K. O., & Ajayi, V. O. (2019). Sensitivity of different physics schemes in the WRF model during a West African Monsoon regime. *Theoretical and Applied Climatology*, *136*(1), 733–751. https://doi.org/10.1007/s00704-018-2538-x

Ghosh, S., & Mujumdar, P. P. (2009). Climate change impact assessment: Uncertainty modeling with imprecise probability. *Journal of Geophysical Research: Atmospheres*, *114*(D18). https://doi.org/10.1029/2008JD011648

Giorgi, F., & Gutowski, W. J. (2015). Regional dynamical downscaling and the CORDEX initiative. *Annual Review of Environment and Resources*, *40*(1), 467–490. https://doi.org/10.1146/annurev-environ-102014-021217

Gleixner, S., Demissie, T., & Diro, G. (2020). Did ERA5 improve temperature and precipitation reanalysis over East Africa? *Atmosphere*, *11*(9), 996. https://doi.org/10.3390/atmos11090996

Glotter, M., Elliott, J., McInerney, D., Best, N., Foster, I., & Moyer, E. J. (2014). Evaluating the utility of dynamical downscaling in agricultural impacts projections. *National Academy of Sciences*, *111*(24), 8776–8781. https://doi.org/10.1073/pnas.1314787111

Gnitou, G. T., Tan, G., Niu, R., & Nooni, I. K. (2021). Assessing past climate biases and the added value of CORDEX-CORE precipitation simulations over Africa. *Remote Sensing*, *13*(11), 2058. https://doi.org/10.3390/rs13112058

Gobiet, A., Suklitsch, M., & Heinrich, G. (2015). The effect of empirical-statistical correction of intensity-dependent model errors on the temperature climate change signal. *Hydrology and Earth System Sciences*, *19*(10), 4055–4066. https://doi.org/10.5194/hess-19-4055-2015

Greenstone, O., & Greenstone, M. (2007). The economic impacts of climate change: Evidence from agricultural output and random fluctuations in weather. *American Economic Review*, *97*(1), 354–385.

Grell, G. A., & Dévényi, D. (2002). A generalized approach to parameterizing convection combining ensemble and data assimilation techniques, *Geophysical Research Letters*, *29*(14), https://doi.org/10.1029/2002GL015311

Gudmundsson, L., Bremnes, J. B., Haugen, J. E., & Engen-Skaugen, T. (2012). Technical note: Downscaling RCM precipitation to the station scale using statistical transformations—A comparison of methods. *Hydrology Earth Systeme Sciences*, *16*, 3383–3390. https://doi.org/10.5194/hess-16-3383-2012

Guo, L.-Y., Gao, Q., Jiang, Z.-H., & Li, L. (2018). Bias correction and projection of surface air temperature in LMDZ multiple simulation over central and eastern China. *Advances in Climate Change Research*, *9*(1), 81–92. https://doi.org/10.1016/j.accre.2018.02.003

Gutjahr, O., & Heinemann, G. (2013). Comparing precipitation bias correction methods for high-resolution regional climate simulations using COSMO-CLM. *Theoretical and Applied Climatology*, *114*(3), 511–529. https://doi.org/10.1007/s00704-013-0834-z

Gutowski, W. J., Decker, S. G., Donavon, R. A., Pan, Z., Arritt, R. W., & Takle, E. S. (2003). Temporal-spatial scales of observed and simulated precipitation in Central U.S. Climate. *Journal of Climate*, *16*(22), 3841–3847. https://doi.org/10.1175/1520-0442(2003)016<3841:TSOOAS>2.0.CO;2

Hagemann, S., Chen, C., Clark, D., Folwell, S., Gosling, S., Haddeland, I., & Wiltshire, A. (2013). Climate change impact on available water resources obtained using multiple global climate and hydrology models. *Earth System Dynamics*, *4*(1), 129–144. https://doi.org/10.5194/esd-4-129-2013

Hatfield, J. L., & Prueger, J. H. (2015). Temperature extremes: Effect on plant growth and development. *Weather and Climate Extremes*, *10*, 4–10. https://doi.org/10.1016/j.wace.2015.08.001

Heinzeller, D., Dieng, D., Smiatek, G., Olusegun, C., Klein, C., Hamann, I., & Kunstmann, H. (2018). The WASCAL high-resolution regional climate simulation ensemble for West Africa: Concept, dissemination, and assessment. *Earth System Science Data*, *10*(2), 815–835. https://doi.org/10.5194/essd-10-815-2018

Heise, E., Lange, M., Ritter, B., Schrodin, R. (2003). Improvement and validation of the multilayer soil model. *COSMO Newsletter 3*:198–203. Retrieved from http://www.cosmo-model.org/content/model/documentation/newsLetters/default

Herger, N., Abramowitz, G., Knutti, R., Angélil, O., Lehmann, K., & Sanderson, B. M. (2018). Selecting a climate model subset to optimize key ensemble properties. *Earth System Dynamics*, *9*(1), 135–151. https://doi.org/10.5194/esd-9-135-2018

Hong, S., Dudhia, J., & Chen, S. (2004). A Revised Approach to Ice Microphysical Processes for the Bulk Parameterization of Clouds and Precipitation, *Monthly Weather Review*, *132*(1), 103-120. Retrieved from https://journals.ametsoc.org/view/journals/mwre/132/1/1520-0493_2004_132_0103_aratim_2.0.co_2.xml

Iizumi, T., Takikawa, H., Hirabayashi, Y., Hanasaki, N., & Nishimori, M. (2017). Contributions of different bias-correction methods and reference meteorological forcing data sets to uncertainty in projected temperature and precipitation extremes. *Journal of Geophysical Research: Atmospheres*, *122*(15), 7800–7819. https://doi.org/10.1002/2017JD026613

Ilori, O. W., & Ajayi, V. O. (2020). Change detection and trend analysis of future temperature and rainfall over West Africa. *Earth Systems and Environment*, *4*(3), 493–512. https://doi.org/10.1007/s41748-020-00174-6

Im, E., Ahn, J., & Jo, S. (2015). Regional climate projection over South Korea simulated by the HadGEM2-AO and WRF model chain under RCP emission scenarios. *Climate Research*, *63*, 249–266. https://doi.org/10.3354/cr01292

Ivanov, M. A., & Kotlarski, S. (2017). Assessing distribution-based climate model bias correction methods over an alpine domain: Added value and limitations. *International Journal of Climatology*, *37*(5), 2633–2653. https://doi.org/10.1002/joc.4870

Ivanov, M. A., Luterbacher, J., & Kotlarski, S. (2018). Climate model biases and modification of the climate change signal by intensity-dependent bias correction. *Journal of Climate*, *31*(16), 6591–6610. https://doi.org/10.1175/JCLI-D-17-0765.1

Jackson, L. S., Marsham, J. H., Parker, D. J., Finney, D. L., Fitzpatrick, R. G. J., Rowell, D. P., & Tucker, S. (2021). The effect of explicit convection on climate change in the West African Monsoon and central West African Sahel rainfall. *Journal of Climate*, 1–42. https://doi.org/10.1175/JCLI-D-21-0258.1

Janjic, Z.I. (1996). The surface layer in the NCEP Eta Model. *Eleventh Conference on Numerical Weather Prediction*, Norfolk, VA, 19-23 August 1996; American Meteorological Society.

Janjic, Z. I., Gerrity, J. P., Jr., & Nickovic, S. (2002). An Alternative Approach to Nonhydrostatic Modeling, *Monthly Weather Review*, *129*(5), 1164-1178. Retrieved from https://journals.ametsoc.org/view/journals/mwre/129/5/1520-0493_2001_129_1164_aaatnm_2.0.co_2.xml

Jie, C., François, P. B., Diane, C., & Marco, B. (2013). Performance and uncertainty evaluation of empirical downscaling methods in quantifying the climate change impacts on hydrology over two North American river basins. *Journal of Hydrology*, *479*, 200–214. https://doi.org/10.1016/j.jhydrol.2012.11.062

Jones, C. D., Hughes, J. K., Bellouin, N., Hardiman, S. C., Jones, G. S., Knight, J., & Zerroukat, M. (2011). The HadGEM2-ES implementation of CMIP5 centennial simulations. *Geoscientific Model Development*, *4*(3), 543–570. https://doi.org/10.5194/gmd-4-543-2011

Kauffeldt, A., Wetterhall, F., Pappenberger, F., Salamon, P., & Thielen, J. (2016). Technical review of large-scale hydrological models for implementation in operational flood forecasting schemes on continental level. *Environmental Modelling & Software*, *75*, 68–76. https://doi.org/10.1016/j.envsoft.2015.09.009

Kirchmeier-Young, M. C., Zwiers, F. W., Gillett, N. P., & Cannon, A. J. (2017). Attributing extreme fire risk in Western Canada to human emissions. *Climatic Change*, *144*(2), 365–379. https://doi.org/10.1007/s10584-017-2030-0

Klein, C., Heinzeller, D., Bliefernicht, J., & Kunstmann, H. (2015). Variability of West African Monsoon patterns generated by a WRF multi-physics ensemble. *Climate Dynamics*, *45*(9), 2733–2755. https://doi.org/10.1007/s00382-015-2505-5

Knox, J., Hess, T., Daccache, A., & Wheeler, T. (2012). Climate change impacts on crop productivity in Africa and South Asia. *Environmental Research Letters*, *7*(3), 034032. https://doi.org/10.1088/2F1748-9326/2F7/2F3/2F034032

Koné, B., Diedhiou, A., Diawara, A., Anquetin, S., Touré, N. E., Bamba, A., & Kobea, A. T. (2020). Influence of initial soil moisture in a regional climate model study over West Africa: Part 1: Impact on the climate mean. *Hydrology and Earth System Sciences Discussions*, *26*, 711–730. https://doi.org/10.5194/hess-2020-112

Lafon, T., Dadson, S., Buys, G., & Prudhomme, C. (2013). Bias correction of daily precipitation simulated by a regional climate model: A comparison of methods. *International Journal of Climatology*, *33*(6), 1367–1381. https://doi.org/10.1002/joc.3518

Lalou, R., Sultan, B., Muller, B., & Ndonky, A. (2019). Does climate opportunity facilitate smallholder farmers adaptive capacity in the Sahel? *Palgrave Communications*, *5*(1), 81. https://doi.org/10.1057/s41599-019-0288-8

Laux, P., Dieng, D., Portele, T., Wei, J., Shang, S., Zhang, Z., & Kunstmann, H. (2021). A high-resolution regional climate model physics ensemble for northern sub-Saharan Africa. *Frontiers in Earth Science*, *9*, 792. https://doi.org/10.3389/feart.2021.700249

Laux, P., Kunstmann, H., & Bárdossy, A. (2008). Predicting the regional onset of the rainy season in West Africa. *International Journal of Climatology*, *28*(3), 329–342. https://doi.org/10.1002/joc.1542

Laux, P., Rötter, R. P., Webber, H., Dieng, D., Rahimi, R., Wei, J., & Kunstmann, K. (2021). To bias correct or not to bias correct? An agricultural impact modelers'? Perspective on regional climate model data. *Agricultural and Forest Meteorology*, *304–305*, 108406. https://doi.org/10.1016/j.agrformet.2021.108406

Lobell, D. B., Schlenker, W., & Roberts, J. C. (2011). Climate trends and global crop production since 1980. *Science*, *333*(6042), 616–620. https://doi.org/10.1126/science.1204531

Maraun, D. (2012). Nonstationarities of regional climate model biases in European seasonal mean temperature and precipitation sums. *Geophysical Research Letters*, *39*(6). https://doi.org/10.1029/2012GL051210

Maraun, D. (2016). Bias correcting climate change simulations—A critical review. *Current Climate Change Reports*, *2*(3), 211–220. https://doi.org/10.1007/s40641-016-0050-x

Maraun, D., Shepherd, T. G., Widmann, M., Zappa, G., Walton, D., Gutierrez, J. M., & Mearns, L. O. (2017). Towards process-informed bias correction of climate change simulations. *Nature Climate Change*, *7*(11), 764–773. https://doi.org/10.1038/nclimate3418

Maraun, D., & Widmann, M. (2018). *Statistical downscaling and bias correction for climate research*. Cambridge & New York, NY: Cambridge University Press.

Mechiche-Alami, A., & Abdi, A. M. (2020). Agricultural productivity in relation to climate and cropland management in West Africa. *Scientific Reports*, *10*(1), 3393. https://doi.org/10.1038/s41598-020-59943-y

Mehrotra, R., & Sharma, A. (2016). A multivariate quantile-matching bias correction approach with auto- and cross-dependence across multiple time scales: Implications for downscaling. *Journal of Climate*, *29*(10), 3519–3539. https://doi.org/10.1175/JCLI-D-15-0356.1

Meyer, J., Kohn, I., Stahl, K., Hakala, K., Seibert, J., & Cannon, A. J. (2019). Effects of univariate and multivariate bias correction on hydrological impact projections in alpine catchments. *Hydrology and Earth System Sciences*, *23*(3), 1339–1354. https://doi.org/10.5194/hess-23-1339-2019

Misra, A. K. (2014). Climate change and challenges of water and food security. *International Journal of Sustainable Built Environment*, *3*(1), 153–165. https://doi.org/10.1016/j.ijsbe.2014.04.006

Monerie, P.-A., Wainwright, C. M., Sidibe, M., & Akinsanola, A. A. (2020). Model uncertainties in climate change impacts on Sahel precipitation in ensembles of CMIP5 and CMIP6 simulations. *Climate Dynamics*, *55*(5), 1385–1401. https://doi.org/10.1007/s00382-020-05332-0

Nangombe, S. S., Zhou, T., Zhang, W., Zou, L., & Li, D. (2019). High-temperature extreme events over Africa under 1.5°C and 2°C of global warming. *Journal of Geophysical Research: Atmospheres*, *124*(8), 4413–4428. https://doi.org/10.1029/2018JD029747

Niang, A., Becker, M., Ewert, F., Dieng, I., Gaiser, T., Tanaka, A., & Saito, K. (2017). Variability and determinants of yields in rice production systems of West Africa. *Field Crops Research*, *207*, 1–12. https://doi.org/10.1016/j.fcr.2017.02.014

Niang, I., Ruppel, O., Abdrabo, M., Essel, A., Lennard, C., Padgham, J., & Urquhart, P. (2014). In V. Barros, et al. (Eds.). Climate change 2014: Impacts, adaptation, and vulnerability. Part B: Regional aspects. Contribution of Working Group II to the Fifth Assessment Report of the Intergovernmental Panel on Climate Change. Cambridge & New York, NY: Cambridge University Press (Nos. 1199-1265).

Nikiema, M., Sylla, M., Ogunjobi, K., Kebe, I., Gibba, P., & Giorgi, F. (2016). Multi-model CMIP5 and CORDEX simulations of historical summer temperature and precipitation variabilities over West Africa. *International Journal of Climatology*, *37*(5), 2438–2450. https://doi.org/10.1002/joc.4856

Nikulin, G., Jones, C., Giorgi, F., Asrar, G., Büchner, M., Cerezo-Mota, R., & Sushama, L. (2012). Precipitation climatology in an ensemble of CORDEX-Africa regional climate simulations. *Journal of Climate*, *25*(18), 6057–6078. https://doi.org/10.1175/JCLI-D-11-00375.1

Noble, E., Druyan, L., & Fulakeza, M. (2014). The sensitivity of WRF daily summertime simulations over West Africa to alternative parameterizations. Part I: African wave circulation. *Monthly Weather Review*, *142*(4), 1588–1608. https://doi.org/10.1175/MWR-D-13-00194.1

Noble, E., Druyan, L., & Fulakeza, M. (2017). The sensitivity of WRF daily summertime simulations over West Africa to alternative parameterizations. Part II: Precipitation. *Monthly Weather Review*, *145*(1), 215–233. https://doi.org/10.1175/MWR-D-15-0294.1

Oettli, P., Sultan, B., Baron, C., & Vrac, M. (2011). Are regional climate models relevant for crop yield prediction in West Africa? *Environmental Research Letters*, *6*(1), 014008. https://doi.org/10.1088/1748-9326/6/1/014008

Ogega, O. M., Gyampoh, B. A., & Mistry, M. N. (2020). Intraseasonal precipitation variability over West Africa under 1.5°C and 2.0°C global warming scenarios: Results from CORDEX RCMs. *Climate*, *8*(12). https://doi.org/10.3390/cli8120143

Ojha, R., Kumar, D. N., Sharma, A., & Mehrotra, R. (2013). Assessing severe drought and wet events over India in a future climate using a nested bias-correction approach. *Journal of Hydrologic Engineering*, *18*(7), 760–772. https://doi.org/10.1061/(ASCE)HE.1943-5584.0000585

Otto, I. M., Reckien, D., Reyer, C. P. O., Marcus, R., Le Masson, V., Jones, L., & Serdeczny, O. (2017). Social vulnerability to climate change: A review of concepts and evidence. *Regional Environmental Change*, *17*(6), 1651–1662. https://doi.org/10.1007/s10113-017-1105-9

Oyerinde, G., Hountondji, F., Lawin, A., Odofin, A., Afouda, A., & Diekkrüger, B. (2017). Improving hydro-climatic projections with bias-correction in Sahelian Niger Basin, West Africa. *Climate*, *5*(1), 8. https://doi.org/10.3390/cli5010008

Panitz, H.-J., Dosio, A., Büchner, M., Lüthi, D., & Keuler, K. (2014). COSMO-CLM (CCLM) climate simulations over CORDEX-Africa domain: Analysis of the ERA-Interim driven simulations at 0.44°and 0.22° resolution. *Climate Dynamics*, *42*(11), 3015–3038. https://doi.org/10.1007/s00382-013-1834-5

Paxian, A., Sein, D., Panitz, H.-J., Warscher, M., Breil, M., Engel, T., & Paeth, H. (2016). Bias reduction in decadal predictions of West African Monsoon rainfall using regional climate models. *Journal of Geophysical Research: Atmospheres*, *121*(4), 1715–1735. https://doi.org/10.1002/2015JD024143

Pendergrass, A. G., & Knutti, R. (2018). The uneven nature of daily precipitation and its change. *Geophysical Research Letters*, *45*(21). 11980–11988. https://doi.org/10.1029/2018GL080298

Piani, C., Weedon, G., Best, M., Gomes, S., Viterbo, P., Hagemann, S., & Haerter, J. (2010). Statistical bias correction of global simulated daily precipitation and temperature for the application of hydrological models. *Journal of Hydrology*, *395*(3), 199–215. https://doi.org/10.1016/j.jhydrol.2010.10.024

Quagraine, K. A., Nkrumah, F., Klein, C., Klutse, N. A. B., & Quagraine, K. T. (2020). West African summer monsoon precipitation variability as represented by reanalysis data sets. *Climate*, *8*(10), 111. https://doi.org/10.3390/cli8100111

Quenum, G. M. L., Klutse, N. A. B., Dieng, D., Laux, P., Arnault, J., Kodja, J. D., & Oguntunde, P. G. (2019). Identification of potential drought areas in West Africa under climate change and variability. *Earth Systems Environment*, *3*(3), 429–444. https://doi.org/10.1007/s41748-019-00133-w

Randall, D., Wood, R., Bony, S., Colman, R., Fichefet, T., Fyfe, J., et al. (2007). Cilmate models and their evaluation. In S. Solomon, D. Qin, M. Manning, Z. Chen, M. Marquis, K. B. Averyt, et al. (Eds.), *Climate change 2007: The physical science basis. Contribution of Working Group I to the Fourth Assessment Report of the Intergovernmental Panel on Climate Change*. Cambridge & New York, NY, Cambridge University Press.

Ritter, B., & Geleyn, J. (1992). A Comprehensive Radiation Scheme for Numerical Weather Prediction Models with Potential Applications in Climate Simulations, *Monthly Weather Review*, *120*(2), 303-325. Retrieved from https://journals.ametsoc.org/view/journals/mwre/120/2/1520-0493_1992_120_0303_acrsfn_2_0_co_2.xml

Rosenzweig, C., Elliott, J., Deryng, D., Ruane, A. C., Müller, C., Arneth, A., & Jones, J. W. (2014). Assessing agricultural risks of climate change in the 21st century in a global gridded crop model intercomparison. *National Academy of Sciences*, *111*(9), 3268–3273. https://doi.org/10.1073/pnas.1222463110

Roudier, P., Ducharne, A., & Feyen, L. (2014). Climate change impacts on runoff in West Africa: A review. *Hydrology and Earth System Sciences*, *18*(7), 2789–2801. https://doi.org/10.5194/hess-18-2789-2014

Saini, R., Wang, G., Yu, M., & Kim, J. (2015). Comparison of RCM and GCM projections of boreal summer precipitation over Africa. *Journal of Geophysical Research: Atmospheres*, *120*(9), 3679–3699. https://doi.org/10.1002/2014JD022599

Salack, S., Abdou Saley, I., & Bliefernicht, J. (2018). Observed data of extreme rainfall events over the West African Sahel. *Data in Brief*, *20*, 1274–1278. https://doi.org/10.1016/j.dib.2018.09.001

Salack, S., Muller, B., Gaye, A. T., Hourdin, F., & Cissé, N. (2012). Analyses multi-echelles des pauses pluviometriques au Niger et au Sénégal. *Science et Changements Planétaires / Sécheresse*, *23*(1), 3–13. https://doi.org/10.1684/sec.2012.0335

Salack, S., Sarr, B., Sangare, S. K., Ly, M., Sanda, I. S., & Kunstmann, H. (2015). Crop-climate ensemble scenarios to improve risk assessment and resilience in the semi-arid regions of West Africa. *Climate Research*, *65*, 107–121. https://doi.org/10.3354/cr01282

Sawadogo, W., Abiodun, B. J., & Okogbue, E. C. (2019). Projected changes in wind energy potential over West Africa under the global warming of 1.5°C and above. *Theoretical and Applied Climatology*, *138*(1), 321–333. https://doi.org/10.1007/s00704-019-02826-8

Schär, C., Ban, N., Fischer, E. M., Rajczak, J., Schmidli, J., Frei, C., & Zwiers, F. W. (2016). Percentile indices for assessing changes in heavy precipitation events. *Climate Change*, *137*(1), 201–216. https://doi.org/10.1007/s10584-016-1669-2

Schlenker, W., & Roberts, M. J. (2009). Nonlinear temperature effects indicate severe damages to U.S. crop yields under climate change. *National Academy of Sciences*, *106*(37), 15594–15598. https://doi.org/10.1073/pnas.0906865106

Schulzweida, U. (2019). *CDO user guide*. https://doi.org/10.5281/zenodo.3539275

Serdeczny, O., Adams, S., Baarsch, F., Coumou, D., Robinson, A., Hare, W., & Reinhardt, J. (2017). Climate change impacts in sub-Saharan Africa: From physical changes to their social repercussions. *Regional Environmental Change*, *17*(6), 1585–1600. https://doi.org/10.1007/s10113-015-0910-2

Sharon, M. G., Adam, M. S., & David, B. L. (2013). Global crop exposure to critical high temperatures in the reproductive period: Historical trends and future projections. *Environmental Research Letters*, *8*(2), 024041.

Sheau, T. N., Fredolin, T., & Liew, J. (2017). Bias correction of global and regional simulated daily precipitation and surface mean temperature over southeast Asia using quantile mapping method. *Global and Planetary Change*, *149*, 79–90. https://doi.org/10.1016/j.gloplacha.2016.12.009

Shiru, M. S., & Park, I. (2020). Comparison of ensembles projections of rainfall from four bias correction methods over Nigeria. *Water*, *12*(11). https://doi.org/10.3390/w12113044

Sidibé, M., Dieppois, B., Eden, J., Mahé, G., Paturel, J.-E., Amoussou, E., & Lawler, D. (2020). Near-term impacts of climate variability and change on hydrological systems in West and central Africa. *Climate Dynamics*, *54*(3), 2041–2070. https://doi.org/10.1007/s00382-019-05102-7

Singh, H., Dube, A., Kumar, S., & Ashrit, R. (2019). Bias correction of maximum temperature forecasts over India during March–May 2017. *Journal of Earth System Science*, *129*(1), 13. https://doi.org/10.1007/s12040-019-1291-6

Sippel, S., Otto, F. E. L., Forkel, M., Allen, M. R., Guillod, B. P., Heimann, M., & Mahecha, M. D. (2016). A novel bias correction methodology for climate impact simulations. *Earth System Dynamics*, *7*(1), 71–88. https://doi.org/10.5194/esd-7-71-2016

Soares, P. M. M., Brito, M. C., & Careto, J. A. M. (2019). Persistence of the high solar potential in Africa in a changing climate. *Environmental Research Letters*, *14*(12), 124036. https://doi.org/10.1088/1748-9326/ab51a1

Stackhouse, P. W., Jr., Gupta, S. K., Cox, S. J., Mikovitz, C., Zhang, T., & Hinkelman, L. (2011). The NASA/GEWEX surface radiation budget release 3.0: 24.5 yr data set. *Gewex News*, *21*(1), 10–12. Retrieved from http://www.gewex.org/resources/gewex-news/

Stevens, B., Giorgetta, M., Esch, M., Mauritsen, T., Crueger, T., Rast, S., et al. (2013). Atmospheric component of the MPI-M Earth System Model: ECHAM6. *Journal of Advances in Modeling Earth Systems*, *5*(2), 146–172. https://doi.org/10.1002/jame.20015

Stouffer, R., Eyring, V., Meehl, G. A., Bony, S., Senior, C., Stevens, B., & Taylor, K. E. (2017). CMIP5 scientific gaps and recommendations for CMIP6. *Bulletin of the American Meteorological Society*, *98*(1), 95–105. https://doi.org/10.1175/BAMS-D-15-00013.1

Sultan, B., Defrance, D., & Iizumi, T. (2019). Evidence of crop production losses in West Africa due to historical global warming in two crop models. *Scientific Reports*, *4*(12834). https://doi.org/10.1038/s41598-019-49167-0

Sultan, B., & Gaetani, M. (2016). Agriculture in West Africa in the twenty-first century: Climate change and impacts scenarios, and potential for adaptation. *Frontiers in Plant Science*, *7*(1262). https://doi.org/10.3389/fpls.2016.01262

Sylla, M., Elguindi, N., Giorgi, F., & Wisser, D. (2016). Projected robust shift of climate zone over West Africa in response to anthropogenic climate change for the late 21st century. *Climatic Change*, *134*(1), 241–253. https://doi.org/10.1007/s10584-015-1522-z

Sylla, M., Giorgi, F., Coppola, E., & Mariotti, L. (2012). Uncertainties in daily rainfall over Africa: Assessment of gridded observation products and evaluation of a regional climate model simulation. *International Journal of Climatology*, *33*(7), 1805–1817. https://doi.org/10.1002/joc.3551

Sylla, M., Giorgi, F., Pal, J., Gibba, P., Kebe, I., & Nikiema, M. (2015). Projected changes in the annual cycle of high-intensity precipitation events over West Africa for the late twenty-first century. *Journal of Climate*, *28*(16), 6475–6488. https://doi.org/10.1175/JCLI-D-14-00854.1

Tall, A., Coulibaly, J., & Diop, M. (2018). Do climate services make a difference? A review of evaluation methodologies and practices to assess the value of climate information services for farmers: Implications for Africa. *Climate Services*, *11*, 1–12. https://doi.org/10.1016/j.cliser.2018.06.001

Tarek, M., Brissette, F., & Arsenault, R. (2020). Uncertainty of gridded precipitation and temperature reference data sets in climate change impact studies. *Hydrology and Earth System Sciences Discussions*, *2020*, 1–32. https://doi.org/10.5194/hess-2020-517

Teutschbein, C., & Seibert, J. (2012a). Bias correction of regional climate model simulations for hydrological climate-change impact studies: Review and evaluation of different methods. *Journal of Hydrology*, *456–457*, 12–29. https://doi.org/10.1016/j.jhydrol.2012.05.052

Teutschbein, C., & Seibert, J. (2012b). Bias correction of regional climate model simulations for hydrological climate-change impact studies: Review and evaluation of different methods. *Journal of Hydrology*, *456*, 12–29. https://doi.org/10.1016/j.jhydrol.2012.05.052

Themeßl, M., Gobiet, A., & Heinrich, G. (2012). Empirical-statistical downscaling and error correction of regional climate models and its impact on the climate change signal. *Climate Change*, *112*(2), 449–468. https://doi.org/10.1007/s10584-011-0224-4

Thorncroft, C. D., Nguyen, H., Zhang, C., & Peyrillé, P. (2011). Annual cycle of the West African monsoon: Regional circulations and associated water vapor transport. *Quarterly Journal of the Royal Meteorological*, *137*(654), 129–147. https://doi.org/10.1002/qj.728

Tiedtke, M. (1989). A Comprehensive Mass Flux Scheme for Cumulus Parameterization in Large Scale Models. *Mon. Monthly Weather Review*, *117*, 1779-1800. https://doi.org/10.1175/1520-0493(1989)117<1779:ACMFSF>2.0

Tiwari, P. R., Kar, S. C., Mohanty, U. C., Dey, S., Sinha, P., Raju, P. V. S., & Shekhar, M. S. (2016). On the dynamical downscaling and bias correction of seasonal-scale winter precipitation predictions over North India. *Quarterly Journal of the Royal Meteorological Society*, *142*(699), 2398–2410. https://doi.org/10.1002/qj.2832

Tobin, I., Bony, S., Holloway, C. E., Grandpeix, J.-Y., Séze, G., Coppin, D., & Roca, R. (2013). Does convective aggregation need to be represented in cumulus parameterizations? *Journal of Advances in Modeling Earth Systems*, *5*(4), 692–703. https://doi.org/10.1002/jame.20047

Todzo, S., Bichet, A., & Diedhiou, A. (2020). Intensification of the hydrological cycle expected in West Africa over the 21st century. *Earth System Dynamics*, *11*(1), 319–328. https://doi.org/10.5194/esd-11-319-

Ulrike, R., Julian, R.-V., Andy, J., Sonja, J. V., Louis, P., Flora, M., & Mark, H. (2016). Timescales of transformational climate change adaptation in sub-Saharan African agriculture. *Nature Climate Change volume*, *6*(6), 605–609. https://doi.org/10.1038/nclimate2947

Vizy, E. K., & Cook, K. H. (2012). Mid-twenty-first-century changes in extreme events over northern and tropical Africa. *Journal of Climate*, *25*, 5748–5767. https://doi.org/10.1175/JCLI-D-11-00693.1

Waongo, M., Laux, P., & Kunstmann, H. (2015). Adaptation to climate change: The impacts of optimized planting dates on attainable maize yields under rainfed conditions in Burkina Faso. *Agricultural and Forest Meteorology*, *205*, 23–39. https://doi.org/10.1016/j.agrformet.2015.02.006

Watanabe, S., Kanae, S., Seto, S., Yeh, P. J.-F., Hirabayashi, Y., & Oki, T. (2012). Intercomparison of bias-correction methods for monthly temperature and precipitation simulated by multiple climate models. *Journal of Geophysical Research: Atmospheres*, *117*(D23). https://doi.org/10.1029/2012JD018192

Weedon, G. P., Balsamo, G., Bellouin, N., Gomes, S., Best, M. J., & Viterbo, P. (2014). The WFDEI meteorological forcing data set: WATCH forcing data methodology applied to ERA-Interim reanalysis data. *Water Resources Research*, *50*(9), 7505–7514. https://doi.org/10.1002/2014WR015638

Wheeler, T. R., Craufurd, P. Q., Ellis, R. H., Porter, J. R., & Vara Prasad, P. V. (2000). Temperature variability and the yield of annual crops. *Agriculture, Ecosystems, & Environment*, *82*(1), 159–167. https://doi.org/10.1016/S0167-8809(00)00224-3

Wilcke, R. A. I., Mendlik, T., & Gobiet, A. (2013). Multi-variable error correction of regional climate models. *Climatic Change*, *120*(4), 871–887. https://doi.org/10.1007/s10584-013-0845-x

Yin, Z., Feng, Q., Yang, L., Deo, R. C., Adamowski, J. F., Wen, X., & Si, J. (2020). Projected spatial patterns in precipitation and air temperature for China northwest region derived from high-resolution regional climate models. *International Journal of Climatology*, *40*(8), 3922–3941. https://doi.org/10.1002/joc

Yira, Y., Diekkrüger, B., Steup, G., & Bossa, A. Y. (2017). Impact of climate change on hydrological conditions in a tropical West African catchment using an ensemble of climate simulations. *Hydrological Earth Systeme Science*, *21*(4), 2143–2161. https://doi.org/10.5194/hess-21-2143-

Zhang, X., Alexander, L., Hegerl, G. C., Jones, P., Tank, A. K., Peterson, T. C., & Zwiers, F. W. (2011). Indices for monitoring changes in extremes based on daily temperature and precipitation data. *Wiley Interdisciplinary Reviews: Climate Change*, *2*(6), 851–870. https://doi.org/10.1002/wcc.147

Zscheischler, J., Fischer, E. M., & Lange, S. (2019). The effect of univariate bias adjustment on multivariate hazard estimates. *Earth System Dynamics*, *10*(1), 31–43. https://doi.org/10.5194/esd-10-31-2019

Zscheischler, J., & Seneviratne, S. I. (2017). Dependence of drivers affects risks associated with compound events. *Science Advances*, *3*(6), e1700263. https://doi.org/10.1126/sciadv.1700263